Journal of Plant Physiology 304 (2025) 154413

Contents lists available at ScienceDirect

Journal of Plant Physiology

journal homepage: www.elsevier.com/locate/jplph

Overexpression of the constitutively-active *AtCPK1* mutant in tobacco plants confers cold and heat tolerance, possibly through modulating abscisic acid and salicylic acid signalling

G.N. Veremeichik *, O.A. Tikhonova, V.P. Grigorchuk, S.A. Silantieva, E.V. Brodovskaya, D.V. Bulgakov, V.P. Bulgakov

Federal Scientific Centre of the East Asia Terrestrial Biodiversity of the Far East Branch of the Russian Academy of Sciences, Vladivostok, 690022, Russia

ARTICLE INFO

Keywords:
Abscisic acid
Calcium-dependent protein kinases
Reactive oxygen species
Nicotiana tabacum
Heat tolerance
Heat shock factors

ABSTRACT

Calcium-dependent protein kinases (CDPKs) are very effective calcium signal decoders due to their unique structure, which mediates substrate-specific $[Ca^{2+}]_{cyt}$ signalling through phosphorylation. However, Ca^{2+}-dependence makes it challenging to study CDPKs. This work focused on the effects of the overexpression of native and modified forms of the *AtCPK1* gene on the tolerance of tobacco plants to heat and cold. We studied the interaction between the calcium and signalling systems of abscisic acid (ABA) at various temperatures. The hormonal state, stress-induced senescence, and expression of important corresponding genes were investigated. We showed that inactivation of the autoinhibitory domain of the modified constitutively active form of AtCPK1 has a positive effect on resistance not only to long-term cold but also to heat. We showed that the constitutively active form of AtCPK1 under nonstressed conditions activated biosynthesis of ABA, but a decrease in ABA content was detected upon heat exposure. On the basis of our results, we can assume that this effect is achieved through the CPK-dependent activation of salicylic acid (SA) signalling. The obtained data shed light on heat-associated molecular processes and support the possibility of using intradomain modifications of CDPK both for comprehensive study of its functional features and as a bioengineering tool.

1. Introduction

Unique spatiotemporal fluctuations in intracellular calcium ions are often involved in the adequate response of plant cells to external stimuli. The concentration of free Ca^{2+} in the cytosol ($[Ca^{2+}]_{cyt}$) in plant cells is between 100 and 200 nM when the cells are at rest, but it can rise quickly when different stimuli are perceived (Costa et al., 2018; Resentini et al., 2021). The term "induced increase in $[Ca^{2+}]_{cyt}$" refers to an analogue signal that exhibits a unique dynamic known as the cytosolic "Ca^{2+} signature" on the basis of the type and strength of the stimulus (Kudla et al., 2010; Resentini et al., 2021). Decoding of $[Ca^{2+}]_{cyt}$ signals is carried out by special enzymes, the activity of which depends on the level of intracellular calcium ions (White and Broadley, 2003). Three main families of $[Ca^{2+}]_{cyt}$ sensors have been found in plants: calmodulin (CaM), calcineurin B-like proteins (CBL), and Ca^{2+}-dependent protein kinases (CDPKs or CPKs). As explained in detail (Yip Delormel and Boudsocq, 2019), compared with CaM and CBL, structure of CDPKs is unique due to ability to mediate substrate-specific $[Ca^{2+}]_{cyt}$ signalling through phosphorylation. In response to external biotic or abiotic stimuli, decoders of Ca^{2+} signals, including CDPK, trigger reactions regulated by stress-related hormones, such as ethylene (ET), jasmonic acid (JA), salicylic acid (SA), and abscisic acid (ABA) (Bredow and Monaghan, 2019). Stress hormones trigger corresponding resistance processes. In addition to activating regulatory mechanisms, CDPKs exert independent effects on terminal transcription factors and enzymes (Bredow and Monaghan, 2019). There are several dozen distinct *CDPK* gene isoforms found in the plant genome (Yip Delormel and Boudsocq, 2019). Different CDPKs have different characteristics, including substrate selectivity, localization, and calcium sensitivity, among many others. These variants allow the involvement of specific CDPK isoforms in numerous cell processes (Yip Delormel and Boudsocq, 2019).

The overexpression of some *CDPK* genes increases plant resistance only to osmotic stress (Huang et al., 2017; Veremeichik et al., 2021b). It is yet unclear how Ca^{2+} and calcium-dependent protein kinases contribute to thermotolerance (Dekomah et al., 2022). Resistance to

* Corresponding author. Federal Scientific Centre of East Asia Terrestrial Biodiversity FEB RAS, Vladivostok, 690022, Russia.
E-mail address: gala-vera@mail.ru (G.N. Veremeichik).

https://doi.org/10.1016/j.jplph.2024.154413
Received 23 August 2024; Received in revised form 18 December 2024; Accepted 20 December 2024
Available online 20 December 2024

short-term, acute cold stress is increased by the overexpression of different *CDPK* gene isoforms (Almadanim et al., 2017; Liu et al., 2018; Lv et al., 2018). Numerous studies have investigated the role of CDPKs in heat tolerance. Studies (Ray et al., 2007; Romeis et al., 2001; Dubrovina et al., 2013; Dong et al., 2020; Veremeichik et al., 2014; Veremeichik et al., 2022b) have demonstrated that some isoforms react to short-term heat stress. Short-term (2–48 h) acute (42 °C) heat stress increases the expression of 4 of the 19 isoforms of the *CDPK* genes of the wild Chinese grape *V. pseudoreticulata* (Zhang et al., 2015). Compared with cultivated soybeans, wild soy presented considerably greater increases in *GmCDPK5* and *GmCDPK10* expression under extreme short-term stress (Veremeichik et al., 2022b). The activation of protective mechanisms in *CDPK*-overexpressing plants in response to short-term heat treatment has also been shown (Tan et al., 2011; Wang and Song, 2014). Under heat stress, AtCPK28 directly phosphorylates the stress marker enzyme APX2, which regulates resistance to heat (Hu et al., 2021). Overexpression of the *SiCDPK7* gene led to an increase in catalase activity the expression level of heat and cold stress-responsive genes in *SiCDPK7*-expressed Arabidopsis and foxtail millet under stress conditions (Wei et al., 2023). However, there is little evidence of a direct increase in heat tolerance in CDPK-overexpressing plants. There are many conflicting data concerning the role of Ca^{2+} in thermotolerance.

This discrepancy can be explained by the dependence of CDPK on intracellular Ca^{2+} levels: at basal $[Ca^{2+}]_{cyt}$ levels, CDPKs are inactivated due to autoinhibition (Dekomah et al., 2022). Autoinhibition of CDPK is a striking example of self-regulation of stress-inducible enzymes, providing the necessary and sufficient level of response in accordance with the level of impact. The structure of CDPK is represented by four domains: the N-terminal variable domain, which is responsible for the localization and specific recognition of the substrate; the Ser/Thr kinase domain; the C-terminal regulatory calmodulin-like domain (CaM-LD), which has conserved calcium-binding motifs; and the J junction domain, which is an autoinhibitory domain that blocks kinase activity in the absence of calcium ions (Bredow and Monaghan, 2019). Autoinhibition of CDPK occurs by blocking the calmodulin-like domain *via* autoinhibitory domain autoinhibition (Dekomah et al., 2022). As part of an *in vitro* study of the subdomain structure of the autoinhibitory domain, Harper (Harper et al., 1994) and Huang (Huang et al., 1996) obtained various mutant forms of the *AtCPK1* gene (GenBank accession number, AT5G04870; http://www.uniprot.org/UniProt/Q06850) of *Arabidopsis thaliana via* site-directed mutagenesis. In those works, studies were carried out only *in vitro*; the function of mutant forms within a plant cell was not studied. However, two mutant forms are of particular interest for studies at the physiological level. The mutant form of KJM4 was inactive regardless of the presence of Ca^{2+} ions. Substitution of 4 amino acid residues in the C-terminal region of the autoinhibitory domain of KJM4 prevents the binding of the CaMLD domain to Ca^{2+}, which leads to complete inactivation of CDPK (Huang et al., 1996). In Harper's work, the mutant form of KJM23 had a six-amino acid substitution in the central part of the autoinhibitory domain, which ensured maximum enzyme activity regardless of Ca^{2+} ions (Harper et al., 1994).

AtCPK1 from *Arabidopsis* has been one of the most studied members since the first evidence of the presence of CDPKs in plant cells (Watillon et al., 1993). Increases in drought and salt tolerance as well as phytoalexin production have been linked to the overexpression of *AtCPK1* (Huang et al., 2017; Shkryl et al., 2011, 2016; Veremeichik et al., 2016, 2019, 2021a, 2021b). Additionally, AtCPK1 controls the generation of reactive oxygen species (ROS) (Xing et al., 2001; Veremeichik et al., 2021a, 2021b). It can also govern cell death by phosphorylating ORE-SARA1/ANAC092 (ORE1), the primary regulator of cell death (Durian et al., 2020a,b). These findings suggest that AtCPK1 is crucial to the defensive state of plant cells. The overexpression of the constitutively active form of the *AtCPK1* gene (AtCPK-KJM23) led to an increase in the yield of specialized metabolites in transgenic cell cultures of various plant species. In these works, it was shown that replacing 6 of the 35 amino acid residues (KJM23) of the CDPK autoinhibitory domain multiplies the effect of AtCPK1 on secondary metabolism, whereas replacing the other 4 amino acid residues (KJM4) abolishes any effect (Shkryl et al., 2011, 2016; Veremeichik et al., 2016, 2019). Moreover, overexpression of the calcium-independent mutant form of *AtCPK1* accelerated tolerance to abiotic stress treatments (Veremeichik et al., 2021a, 2021b). Salt tolerance can be increased by up to 80% by inactivating the autoinhibitory domain compared to plants expressing the native *AtCDPK1* gene (Veremeichik et al., 2021b). The simultaneous activation of secondary metabolism and tolerance to abiotic stress was demonstrated in *AtCPK1*-transformed cell cultures of *R. cordifolia* (Veremeichik et al., 2021a). This work shows for the first time that the expression of *AtCPK1* can improve heat tolerance. In addition to increased tolerance to cold and salt, the mutant calcium-independent form of *AtCPK1* exhibited strong tolerance to long-term high--temperature treatment (Veremeichik et al., 2021a).

Temperature stress triggers leaf senescence by affecting endogenous signal molecules that regulate leaf senescence. Among these factors, ABA functions as a link between oxidative damage to the cellular structure and the response of signalling molecules to abiotic stress during leaf senescence (Asad et al., 2019). Senescence is regulated coordinately through senescence-associated genes (SAGs), which play a role in macromolecule degradation and reactions to diverse environmental signals. Moreover, SAGs provide extensive signalling crosstalk between the senescence process and stress responses (Lim et al., 2007). ORE1-SAG12 is strongly regulated through ABA signalling (Matallana-Ramirez et al., 2013). In addition to ethylene, ABA is one of the most effective plant hormones for promoting initial leaf senescence (Zacarias and Reid, 1990; Lee et al., 2011). Increases in endogenous ABA have been shown to coincide with leaf senescence, whereas genes involved in ABA signalling are induced earlier during senescence (Breeze et al., 2011). The ABA signalling system consists of a complex of kinases and phosphatases (Chinnusamy et al., 2010). In response to stress, calcium channels are activated, resulting in the activation of messengers that activate the expression of genes encoding enzymes involved in ABA biosynthesis, such as 9-cis-epoxycarotenoid dioxygenase, NCED (Ng et al., 2014). Under stress-induced conditions, excess ABA binds to phosphatases, allowing kinases to trigger cascades of response reactions. In addition to the ABA kinase system, phosphatases also block the function of calcium messengers to reduce stress-induced ABA levels (Roychoudhury et al., 2013). On the other hand, chlorophyll degradation, as a reaction of hypersensitivity and part of programmed cell death (PCD), is also regulated through the ACCELERATED CELL DEATH 6 protease ACD6 (Rate et al., 1999). ACD6 is a key component of the feedback regulatory loop involved in salicylic signalling. By blocking the main manifestations of systemic acquired resistance (SAR), ACD6 initiates stress-induced senescence. Moreover, SA also blocks the effects of ACD6 (Rate et al., 1999). Previous studies have demonstrated that CPK1 activates the salicylic acid signalling system (Coca and San Segundo, 2010; Bredow and Monaghan, 2019), and its constitutively active form also induces the expression of SAR-associated proteins (Veremeichik et al., 2023a). The overexpression of the mutant constitutively active isoform of the *AtCPK1* gene has a significant effect on reactive oxygen species (ROS) metabolism (Veremeichik et al., 2021a, 2021b). ROS are among the key regulatory tools used by plant cells. The ROS signalling system is interconnected with other signalling systems, such as the auxin, ABA, and SA signalling systems (Mittler et al., 2022). Moreover, these signalling systems can modulate each other to ensure survival and reproduction, depending on the conditions (Mittler et al., 2022).

The present study aimed to verify two hypotheses: i) KJM23 mutations in the AtCPK1 junction enhance thermotolerance in plants, and ii) KJM4 mutations disable recombinant AtCPK1. We used transgenic tobacco plants (*Nicotiana tabacum* L. var Xanthi) for the analyses. The ease of transformation and plant regeneration of tobacco make it one of the most convenient plants for transgenic studies (Horsch et al., 1985). In the present work, we studied the effects of the transformation of native

and modified forms of the *AtCPK1* gene on plant resistance to long-term temperature stress, both cold and heat. Moreover, we examined the role of CPK in the early response of the ABA signalling system to heat stress. We clarified the role of CPK in the regulation of heat-induced ABA-dependent senescence processes.

2. Materials and methods

2.1. Plant materials

Previously obtained transgenic tobacco plants were used in the present work (Veremeichik et al., 2021b). For the experiments, we used clonally cultivated plantlets of *Nicotiana tabacum* L. (cv Xanthi): WT as the control and *AtCPK1*-transformed CPK1-OE (plants transformed with the native form of the *AtCPK1* gene, construction pPZP-RCS2-nptII/Ak), KJM4-OE (plants transformed with the nonactive form of the *AtCPK1* gene, construction pART27/*AtCPK1*-KJM4), and KJM23-OE (plants transformed with the active form of the *AtCPK1* gene, construction pART27/*AtCPK1*-KJM23) as described previously (Harper et al., 1994; Huang et al., 1996; Shkryl et al., 2016). The expression level of the *AtCDPK1* gene in the transgenic tobacco plants was the same (Veremeichik et al., 2021b). The control and transgenic plants were clonally cultivated (micropropagated) *in vitro* on MS agar media (Murashige and Skoog, 1962). The following conditions were used for cultivation: temperature, 24/22°C; photoperiod, 16/8 h; illumination in the daytime, 3000–5000 lux of luminescent lamps (near 150 μmol $m^{-2}s^{-1}$); humidity, 70%; and 30-day subculture intervals. Seeds of the third generation (T3) of transgenic *N. tabacum* plants were obtained for germination tests under stress conditions. A resistance test to the selective antibiotic kanamycin was performed to confirm the 100% presence of transgenic homozygotes. The sterilized seeds were germinated on MS/2 media supplemented with 1000 or 2000 mg/L kanamycin. After 5 days, all the plants had germinated; after 10 days, the non-transgenic control plants died, while the growth of the transgenic plants continued (Suppl. Fig. 1).

2.2. Experimental design

Cold treatment. The untransformed control clonally cultivated plantlets of *N. tabacum* (designated WT) and *AtCPK1*, *AtCPK1-KJM4-*, and *AtCPK1-KJM23*-transgenic plantlets of *N. tabacum* (CPK1-OE, KJM4-OE, and KJM23-OE, respectively) were clonally cultivated (micropropagated) in glass tubes *via* MS/2 media supplemented with 10 g/L sucrose (Murashige and Skoog, 1962) in a climate chamber (KS-200, Russia) as described above. The effects of long-term cold stress on the growth of the control WT and transgenic CPK1-OE, KJM4-OE, and KJM23-OE plants were investigated by cultivating them at a low temperature (12 °C) for 30 days. Samples were harvested from 30-day-old plantlets and weighed. To study the germination of normal and transgenic seeds, sterile paper discs soaked in distilled water were added to 12-well plates. Seeds of WT and transgenic plants were harvested from parent plants that grew together under the same conditions and were used immediately and stored at room temperature in the dark. The conditions of germination were as follows: temperature, 24/22°C (control conditions) or 12°C (cold stress); photoperiod, 16/8 h; illumination in the day, 3000–5000 lux of the luminescent lamps (near 150 μmol $m^{-2}s^{-1}$); humidity, 70%. Green cotyledons of all the analysed tobacco lines under control conditions were observed on the 3rd day; after 14 days, the results of the experiments were photographed. Both types of cold stress experiments were repeated three times.

Heat treatment. The effects of heat stress on the growth of control and transgenic *N. tabacum* plants were investigated using control and transgenic tobacco plants growing in soil with regular watering under the same conditions: photoperiod, 16/8 h; illumination during the day, 3000–5000 lux of the luminescent lamps (near 150 μmol $m^{-2}s^{-1}$); humidity, 70%. Two types of experiments were performed: seeds were germinated and grown for 20 and 30 days under control conditions (24 °C), followed by slight heat exposure (36 °C for 20 days) and intense heat exposure (42 °C for 20 days). The corresponding control conditions were 40 and 50 days under the control temperature (24 °C). After the stress treatments, the experimental plants were photographed, and the relative lengths of the shoots under heat exposure (%) were measured. Both types of heat stress experiments were repeated three times.

Molecular analysis. To analyse heat-induced ABA accumulation and determine gene expression, the following experiments were performed. Forty-day-old clonally cultivated normal (WT) and transformed tobacco plants were transferred to 4 °C and 42 °C for 1 h. RNA, or ABA, was extracted immediately. In this work, we used three independent lines of control plants and each type of transgenic plant.

2.3. HPLC-DAD-ESI-MS(/MS) conditions

2.3.1. Chemicals

LC–MS-grade acetonitrile and methanol were acquired from Merck (Darmstadt, Germany). MS-grade formic acid was acquired from Sigma Aldrich (Steinheim, Germany). Deionized water was obtained using a Milli-Q Simplicity water purification system (Millipore, Molsheim, France). Analytical standards of indole-3-acetic acid (IAA), ABA, and SA were obtained from Sigma–Aldrich (St. Louis, MO, USA).

2.3.2. HPLC–MS/MS analysis and quantification of plant hormones

For the quantification of plant hormones, sample preparation and analysis were performed as described previously with the same parameters (Veremeichik et al., 2022b). A Shimadzu LC-30AD HPLC system coupled with a Shimadzu LCMS-8060 triple quadrupole mass spectrometer (Kyoto, Japan) equipped with an electrospray ionization interface was used for analysis. A Shimpack ODSII column (75 × 2 mm i.d., 2.2 μm particle size) (Shimadzu, Duisburg, F.R. Germany) was used at 45 °C. All important parameters of MRM and calibration curves necessary for HPLC–MS/MS analysis are summarized in Supplementary Table 1.

2.3.3. HPLC–MS/MS analysis and quantification of the breakdown products of chlorophyll

Phyllobilin extraction was performed as described previously (Veremeichik et al., 2023b). The reversed-phase high-performance liquid chromatography with diode array detection and electrospray ionization mass spectrometry (RP-HPLC-DAD-ESI-MS/MS^2) method was applied for chlorophyll catabolite determination using a 1260 Infinity analytical HPLC system (Agilent Technologies, Santa Clara, California, USA) interfaced with an ion trap mass spectrometer Bruker HCT ultra PTM Discovery System (Bruker Daltonik GmbH, Bremen, Germany). The separation was carried out using an analytical Zorbax C18 column (150 mm, 2.1 mm i.d., 3.5 μm; Agilent Technologies, USA) with a flow rate of 0.2 ml/min and a column temperature of 40 °C. The mobile phase consisted of a gradient elution of 0.1% aqueous acetic acid (A) and acetonitrile (B). A binary gradient with A and B was installed, starting with 10% B and reaching 60% B at 40 min. UV/Vis spectra were recorded with a DAD in the range of 200–600 nm, and chromatograms were obtained at a wavelength of 312 nm. The MS data were collected in positive ion mode with a range of m/z 100–1200. The following settings were used: the drying gas (N_2) flow rate was 8.0 L/min, the nebulizer gas (N_2) pressure was 175 kPa, the capillary voltage was kept at −4.0 kV, and the drying gas temperature was 325 °C. Tandem mass spectra were acquired in auto-MS^2 mode (smart fragmentation) by increasing the collision energy. The fragmentation amplitude was set to 1 V.

High-resolution mass spectrometry (HRMS) was carried out *via* an LCMS-IT-TOF tandem mass spectrometer (Shimadzu, Japan), including an LC-20AD Prominence (Shimadzu, Japan), and an ion trap/time-of-flight mass spectrometer. The mass spectra were recorded using electrospray ionization with simultaneous negative and positive ion detection and a resolution of 12,000. The following settings were used: the

range of m/z detection was 400–1,200, the drying gas (N_2) pressure was 150 kPa, the nebulizer gas flow rate was 1.5 L/min, the ion source potential changed from −3.8 to 4.5 kV, and the interface temperature was 200 °C.

2.4. ABA ELISA

For the ELISA of the baseline and heat-induced ABA contents, sample preparation was performed according to previously described methods (Veselov et al., 1992). Heat-treated (42°C for 1 h) and untreated 40-day-old plants grown *in vitro* were powdered with liquid nitrogen and immediately weighed to 300 mg. Extraction was performed in 1 ml of 80% ethanol for 16 h at 4 °C. After incubation, the extracts were centrifuged, and the supernatant was dried (Concentrator Plus, Eppendorf). The dried pellet was dissolved in 1 ml of water acidified with HCl (pH 2–3). Then, ABA was concentrated twice with diethyl ether. The ether phase was dried; the pellet was dissolved in 50 µl of 80% ethanol and used immediately for the ELISA. ELISA was performed *via* an ELISA Kit for Abscisic Acid (Cloud-Clone Corp., China) according to the manufacturer's instructions. The samples were analysed in a 96-well plate using a spectrophotometer (Benchmark Plus Microplate Reader, Bio-Rad, USA) at a wavelength of 450 nm. The results were obtained from a calibration curve constructed according to the optical density of a standard diluted to concentrations of 1.23, 3.70, 11.11, and 33.33 ng/ml. The analysis of ABA content was repeated three times.

2.5. Analysis of gene expression

Total DNA extraction, total RNA extraction, and first-strand cDNA synthesis were performed as described previously (Veremeichik et al., 2019). We used the Actin (Veremeichik et al., 2021b) and elongation factor (Baek et al., 2017) genes from *N. tabacum* as reference genes for real-time PCR analysis. The oligonucleotide pairs used for analysis of *NtHSF* (heat shock factor) gene expression were described previously (Veremeichik et al., 2021b). The oligonucleotide pairs used for analysis of *the NtNCEDs, NtSAG12*, and *NtACD6* genes are listed in Supplementary Table 2. Under the following conditions, PCR and real-time PCR experiments were carried out as previously described (Veremeichik et al., 2019) in a 10 µl volume comprising 1 µl of the diluted cDNA sample and 300 nM of each primer. In a 96-well reaction plate, 3 min at 96 °C was followed by 35 cycles of 15 s at 96 °C and 30 s at 60 °C. Three technical replicates were evaluated for every biological replicate, and two biological replicates were used for the analysis. To confirm that there was no contamination, qPCR analysis was performed with both the RNA-RT and no-template controls. At the end of each run, we employed melting curve analysis to establish the lack of primer−dimer artefacts or nonspecific products. The software CFX Manager was used to analyse the data.

2.6. Statistical analysis

All values were represented *via* Statistica 10.0 (StatSoft Inc., USA) as the mean ± SE. A significance threshold of $P < 0.05$ was applied to the differences. ANOVA and multiple comparisons were used to compare data across different groups, and Student's *t*-test was used to analyse data between two independent categories. For the intergroup comparisons, Fisher's protected least significant difference (PLSD) post hoc test was used.

3. Results

3.1. Steady-state levels of major plant hormones in AtCPK1 transgenic N. tabacum plants

We studied the effects of the overexpression of the native and modified forms of the *AtCPK1* gene on the intracellular levels of IAA, ABA, and SA in *N. tabacum* plants. The contents of IAA, ABA, and SA in the extracts of 40-day-old *in vitro* cultivated plants were determined using HPLC-DAD-HRMS/MS2 (high-performance liquid chromatography with a diode array detector in combination with a high-resolution tandem mass spectrometer). The WT tobacco plants contained twice as much SA (up to 0.8 ng/g fresh weight) as IAA (up to 0.4 ng/g fresh weight). The amount of ABA was within 40 ng/g of fresh weight in the WT plants, which was 100 times greater than the content of IAA (Fig. 1). By comparing the contents of IAA, ABA, and SA in the WT and transgenic plants, we showed that the transformation of both the inactive mutant (KJM4-OE) and native forms of the *AtCPK1* gene had no effect on the hormonal status of the transgenic plants compared with that of the control plants. Moreover, we observed a significant increase in the content of ABA in KJM23-OE plants. The ABA content in the KJM23-OE plants reached 50 ng/g of fresh tissue, which was 20% greater than the ABA content in the WT plants (Fig. 1).

Both endogenous and exogenous ABA are known to inhibit seed germination (Kang et al., 2015). Therefore, the germination of WT and *AtCPK1*-transgenic *N. tabacum* seeds was studied. Seeds of the third generation (T3) of transgenic *N. tabacum* plants were obtained. A kanamycin assay was performed to confirm the presence of 100% of the transgenic homozygotes (Suppl. Fig. 1). To avoid biotic and abiotic effects, the seeds were grown under sterile, controlled *in vitro* conditions. The percentage of germination and the length of the cotyledons were recorded starting from the 4th day and every 2 days until the 10th day. In a series of experiments, 70% of the seeds of the WT plants and KJM4-OE plants germinated on the 4th day, with the length of the cotyledons being 3–4 mm. On the 6th day, 80–90% of the seeds germinated, and the length of the cotyledons ranged from 7 to 8 mm. On the 8th day, the length of the cotyledons exceeded 10 mm and doubled by the 10th day (Fig. 2). The transformation of the native *AtCPK1* gene had a slight inhibitory effect on the germination rate on the 4th day; however, further differences were not found. The overexpression of *AtCPK1*-KJM23 led to significant inhibition of germination. The germination rate of the KJM23-OE seeds was equal to that of the WT plants up to the 10th day, and the length of the cotyledons was equal to that on the 10th day. Only on the 6th day did the percentage of germination of KJM23-OE plants reach the level of that of the control plants on the 4th day. On the 8th day, the percentage of germination of the KJM23-OE seeds was equal to that of the control. The length of the KJM23-OE cotyledons was equal to that of the control cotyledons only on the 10th day. Thus, the delay in the germination of *N. tabacum* plants transformed with *AtCPK1*-KJM23 corresponds to an increase in the level of endogenous ABA.

3.2. Steady-state and ABA-induced chlorophyll degradation in AtCPK1-transgenic N. tabacum plants

Both exogenous and endogenous ABA positively regulates natural aging processes and stress-induced senescence. Moreover, plants with high levels of endogenous ABA are more sensitive to exogenous ABA, which manifests as more intense yellowing of the leaves (Ren et al., 2018). Moreover, AtCPK1 directly interacts with the senescence-associated protein ORE1 (Durian et al., 2020a,b). We analysed the contents of important indicators of senescence, such as the products of chlorophyll degradation and nonfluorescent catabolites, nonfluorescent chlorophyll katabolites/dioxobilin type, and NCC/DNCC (Pérez-Gálvez and Roca, 2017; Christ et al., 2013, 2016). NCC/DNCC are markers of aging and stress-induced senescence (Lim et al., 2007; Moser et al., 2020). To identify the breakdown products of chlorophyll, the leaves of *N. tabacum* plants grown under control unstressed conditions were senesced as described previously (Christ et al., 2013). The identification of the target compounds was based on analysis of their retention time (Rt) and ultraviolet and mass spectrometric data and comparison of the same parameters with literature data (Berghold et al., 2004).

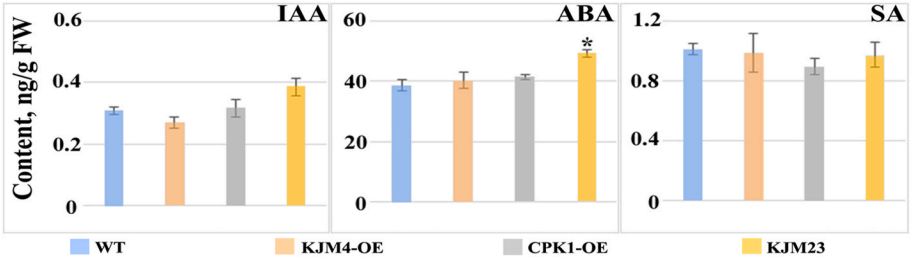

Fig. 1. Determination of the contents of indoleacetic acid (IAA), abscisic acid (ABA), and salicylic acid (SA) in *N. tabacum* plants. The amounts of IAA, ABA, and SA (ng/g fresh tissue) were determined using HPLC-DAD-HRMS/MS2 in 40-day-old tobacco plants: control (WT), transformed native (CPK1-OE), mutant inactive (KJM4-OE), and constitutively active (KJM23-OE) forms of the *AtCPK1* gene. The data were obtained from 6 independent experiments and are presented as the mean ± standard error of the mean. Asterisks above the error bars indicate statistically significant mean differences ($P < 0.05$, Fisher's LSD).

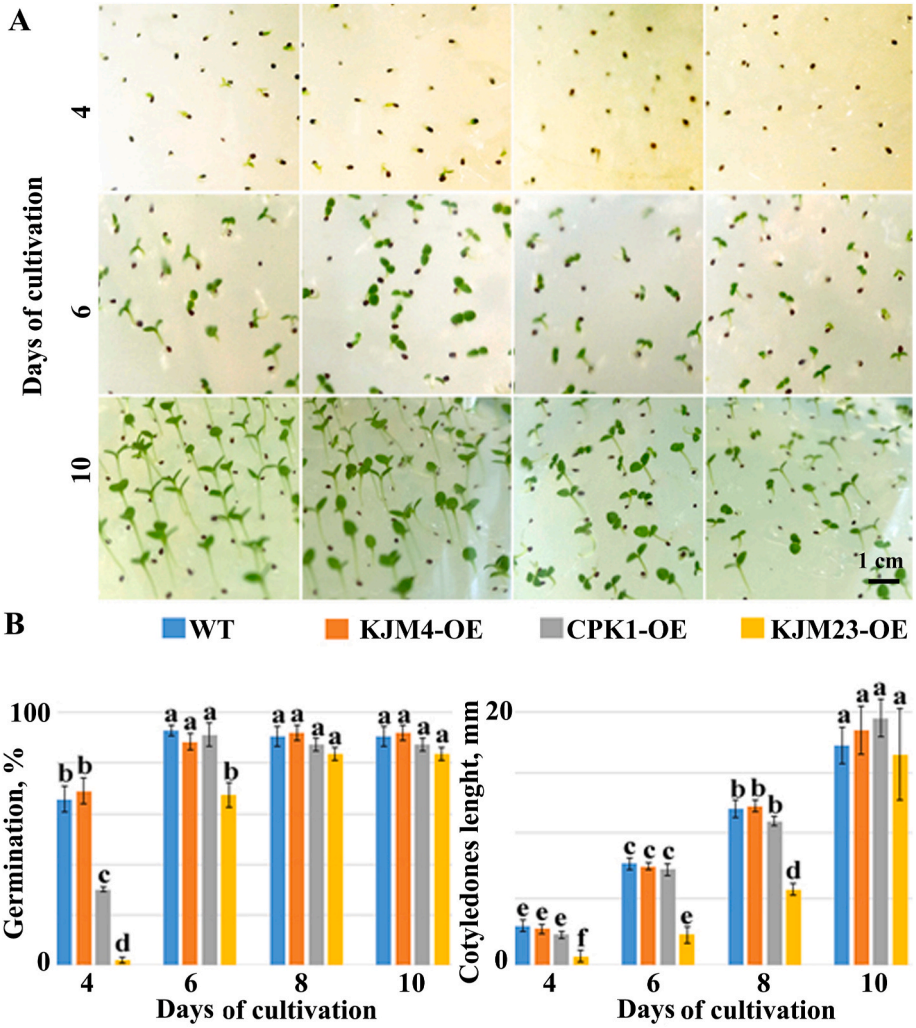

Fig. 2. Effects of the overexpression of native and mutant forms of the *AtCPK1* gene on the germination of *N. tabacum* seeds. Seeds of the control (WT), transformed native (CPK1-OE), mutant inactive (KJM4-OE), and constitutively active (KJM23-OE) *AtCPK1* gene plants were sterilely germinated on MS/2 agar media for 10 days. The results were recorded on the 4th, 6th, 8th, and 10th days. The cotyledons were photographed (**A**), and the percentage and length (mm) of the seedlings were determined (**B**). The data were obtained from 3 independent experiments and are presented as the mean ± standard error of the mean. The different letters above the error bars indicate statistically significant differences ($P < 0.05$, Fisher's LSD).

The artificial senescence of tobacco leaves was used to study the breakdown products of chlorophyll. An analytical HPLC-UV/Vis-MS (MS^2) method was used to identify the compounds whose abundances increased during leaf senescence. Thus, two colourless compounds with characteristic UV/Vis absorbance profiles of nonfluorescent chlorophyll catabolites (NCCs) were detected (Fig. 3A and B). The first compound, with Rt = 23.8 min, was protonated $[M+H]^+$ at *m/z* 807.3430 (error, 1.7 ppm) and more deprotonated $[M-H]^-$ at *m/z* 805.3329 (error, 2.7 ppm) according to high-resolution mass spectrometry and was determined to be $C_{41}H_{50}N_4O_{13}$. Additionally, the second compound with Rt = 25.1 min was defined as $C_{44}H_{52}N_4O_{16}$ ($[M+H]^+$ at *m/z* 893.3432 with an error of 3.3 ppm and $[M-H]^-$ at *m/z* 891.3317 with an error of 1.1 ppm). The MS^2 fragmentation patterns of the protonated molecules $[M+H]^+$ of both compounds were the most consistent (Fig. 3, C). The

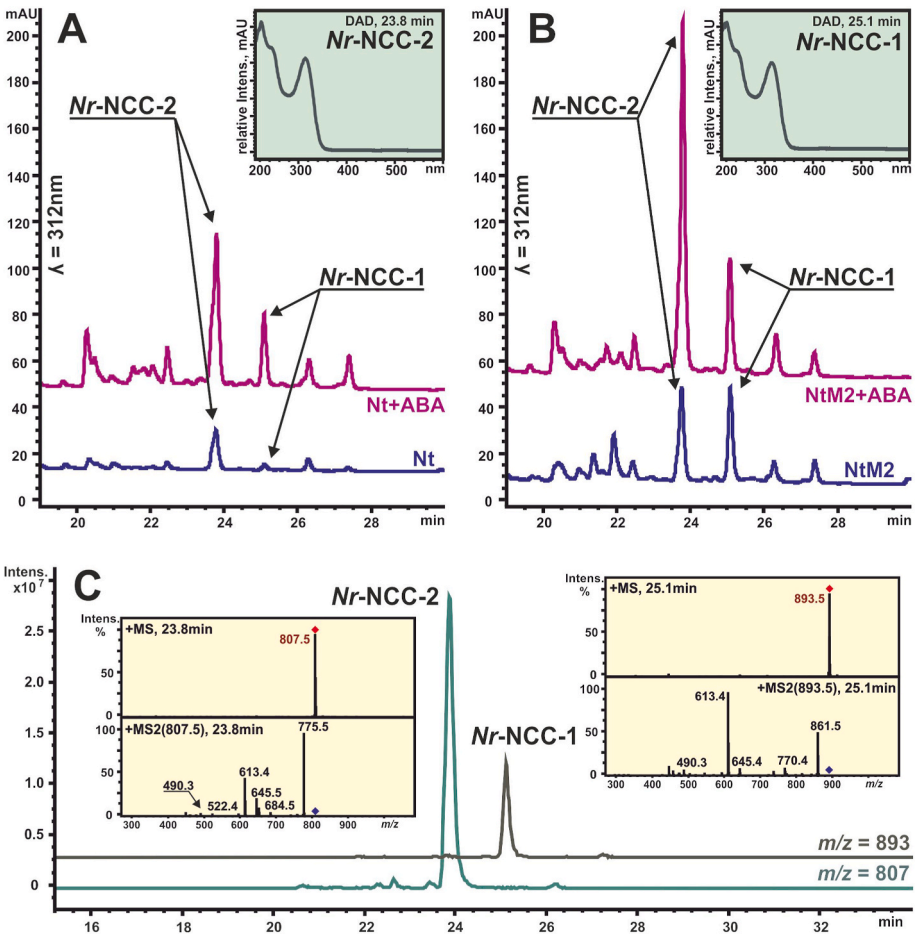

Fig. 3. HPLC-DAD-HRMS/MS2 identification of NCC/DNCC in extracts of 40-day-old *N. tabacum* plants.

characteristic losses of 32 Da (due to the methyl ester) and 123 Da (due to C_7H_9NO – loss of ring A) were observed in both cases (Berghold et al., 2004): signals with *m/z* 775 and 684 for the first compound and *m/z* 861 and 770 for the second one, respectively. Notably, fragment ions at *m/z* 645 and 613 were detected for both compounds and were formed by the elimination of the hexoside residues $[(M + H)\text{-}162]^+$ and $[(M + H)\text{-}32\text{-}162]^+$ from the first compound and the elimination of the malonylated sugar moiety $[(M + H)\text{-}248]^+$ and $[(M + H)\text{-}32\text{-}248]^+$ from the second compound, respectively. The first compound was identified as *Nr*-NCC-2, and the second was identified as its malonylated derivative, *Nr*-NCC-1, as previously shown (Berghold et al., 2004). Quantification calculations were based on differences in the areas of the analysed peaks (Fig. 3).

For analysis, 40-day-old WT and transgenic *N. tabacum* plants grown *in vitro* were used. We studied the steady-state levels of NCC/DNCC as indicators of the intensity of natural aging processes and ABA-induced aging. The plants were sprayed with an ABA solution (5 mM) on the 33rd day of growth and analysed at 7 days after treatment. Three

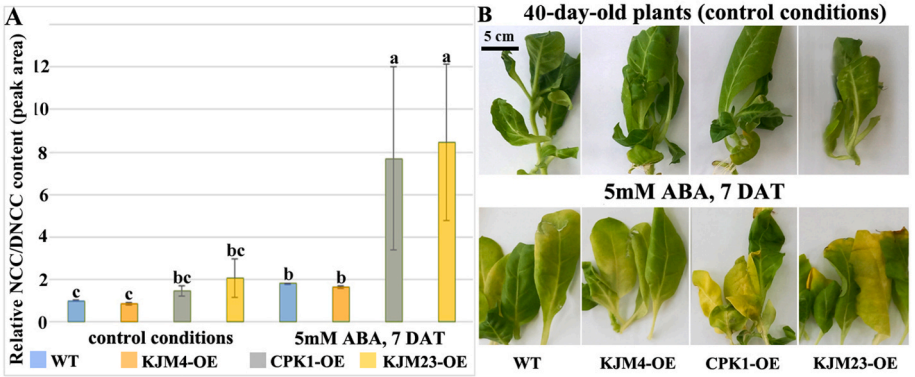

Fig. 4. Effect of the overexpression of native and mutant forms of the *AtCPK1* gene on the content of NCC/DNCC chlorophyll catabolites in *N. tabacum* plants. **A** — Relative content of NCC/DNCC in extracts of 40-day-old tobacco plants: control (WT), transformed native (CPK1-OE), mutant inactive (KJM4-OE), and constitutively active (KJM23-OE) forms of the *AtCPK1* gene. **B** — Plants grown *in vitro* under controlled conditions (top) and treated with a 5 mM ABA solution for 7 days (bottom). The data were obtained from 3 independent experiments and are presented as the mean ± standard error of the mean. The different letters above the error bars indicate statistically significant differences ($P < 0.05$, Fisher's LSD).

independent experiments were conducted using two independent clones of transgenic plants for each variant. The analysis revealed that the relative NCC/DNCC content did not differ between the WT control plants and KJM4-OE plants. ABA treatment reliably increased the relative NCC/DNCC ratio, which is associated with common leaf yellowing (Fig. 4). Moreover, the transformation of the native and KJM23 forms of the *AtCPK1* gene led to an increase in the relative content of NCC/DNCC. Statistical analysis of the data set revealed that the NCC/DNCC content in CPK1-OE and KJM23-OE plants was not markedly different from that in WT plants under control conditions or after exposure to ABA. CPK1-OE and KJM23-OE plants grown under control conditions for 40 days also did not differ from the WT plants. However, a tendency toward increased NCC/DNCC content was observed in all the experiments carried out. Compared with those of the WT plants, the leaves of the CPK1-OE and KJM23-OE plants were markedly yellow after 7 days of exposure to ABA. The relative NCC/DNCC content was more than four times greater in CPK1-OE and KJM23-OE plants than in WT plants (Fig. 4A and B).

3.3. Tolerance of N. tabacum plants transformed with native and modified AtCPK1 genes to long-term cold treatment

The role of *AtCPK1* in osmotic stress tolerance has been previously shown (Huang et al., 2017, 2017b). However, there are no data describing the effects of *CDPK* gene overexpression on tolerance to long-term cold or heat treatment. Moreover, the crosstalk between ABA and cytosolic Ca^{2+} in the temperature stress response is still unclear (Li et al., 2020). Next, we investigated the effects of the expression of the native and modified forms of the *AtCPK1* gene on cold and heat tolerance in tobacco plants.

To determine tolerance to low temperatures, the plants were clonally cultivated (micropropagated) *in vitro* at a low temperature (12 °C) for 30 days (Fig. 5, A). We showed that under low temperature, biomass accumulation of WT plants was reduced to 25% of the untreated wild type (Fig. 5). Similarly, low temperature affected the growth of KJM4-OE plants (Fig. 5). The overexpression of the native form of the *AtCPK1* gene slightly increased cold tolerance. The growth of the CPK1-OE plants was inhibited less than threefold. (Fig. 5). Inactivation of the junction domain in the constitutively active AtCPK1-KJM23 mutant enhanced this effect. The inhibitory effect of cold on the growth and biomass accumulation of KJM23-OE plants was less than 50%. When exposed to low temperatures, the CPK1-OE and KJM23-OE plants presented more voluminous rosettes and shortened stems (Fig. 5).

Next, we studied the effects of cold on the germination of *N. tabacum* WT plants and plants transformed with native and modified forms of the *AtCPK1* gene. The seeds were sterilely germinated for 10 days in 12-well plates on wet filter paper. Low temperature (12 °C) inhibited the germination of WT KJM4-OE plants by 90%, while the cotyledons grew to approximately 1/4 of the height of untreated wild-type plants (Fig. 5, C). The germination of the CPK1-OE plants at low temperatures was inhibited by more than 60%, and the length of the cotyledons decreased by more than 2-fold (Fig. 5C and D). No significant inhibitory effect of low temperature on the germination of KJM23-OE seeds was found. A slight decrease in cotyledon length of only 10% was noted (Fig. 5C and D).

3.4. Tolerance of N. tabacum plants transformed with native and modified AtCPK1 genes to heat shock and long-term heat treatment

We investigated the effects of long-term slight and intense heat treatments on the growth of the transgenic plants. For slight heat treatment, the WT and transgenic plants were grown in soil at a controlled temperature (24 °C) for 20 days. Twenty-day-old WT and transgenic *N. tabacum* plants were subjected to 20 days of exposure to slight heat stress at 36 °C (Fig. 6). More intense heat treatment was performed on 30-day-old plants (Fig. 7) because younger plants cannot withstand an increase in temperature up to 42 °C. After 20 days of heat treatment, the shoots were photographed, and their length was measured. We showed that both slight (36 °C) and intense (42 °C) heat treatments significantly inhibited the growth of the WT plants by 50% and 60%, respectively (Figs. 6 and 7). Moreover, intense heat exposure caused leaf yellowing, which is associated with stress-induced

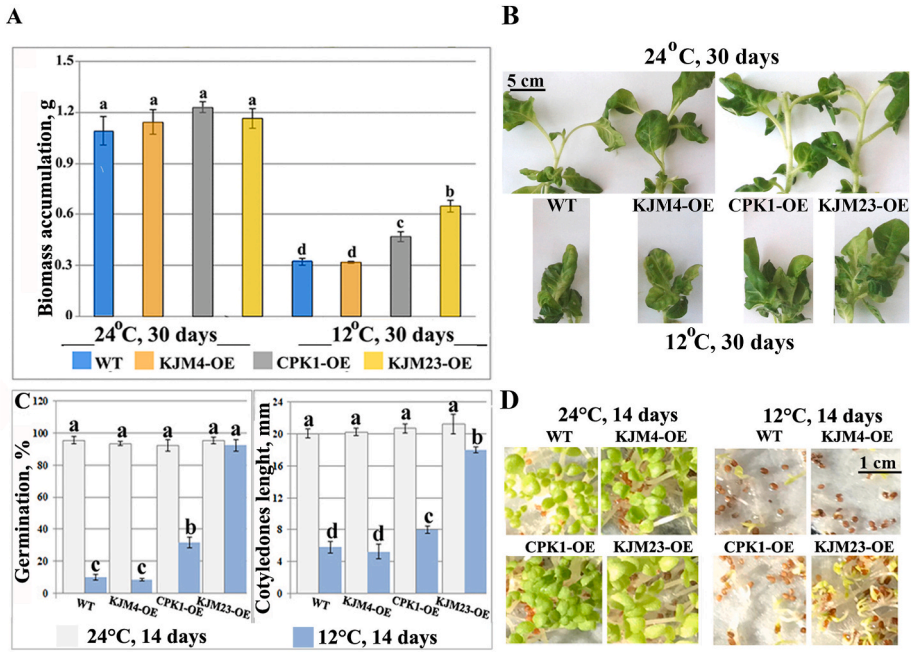

Fig. 5. Effects of low temperature (12 °C) on the growth of *N. tabacum* plants. Biomass accumulation (**A**) and morphology (**B**) of 30-day-old tobacco plants under unstressed conditions (24 °C) and at low temperature (12 °C) for 30 days: control (WT), transformed native (CPK1-OE), mutant inactive (KJM4-OE), and constitutively active (KJM23-OE) forms of the *AtCPK1* gene. The effects of low temperature (12 °C) on the germination (%), length (mm) (**C**), and morphology (**D**) of the cotyledons were determined after 10 days of treatment. The data were obtained from three independent experiments with 10 replicates and are presented as the mean ± standard error of the mean. The different letters above the error bars indicate statistically significant differences ($P < 0.05$, Fisher's LSD).

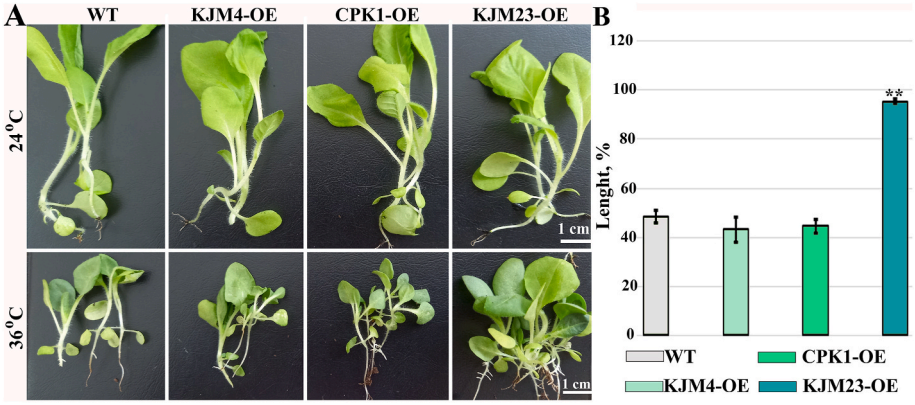

Fig. 6. Effects of moderate heat stress on the growth of *N. tabacum* plants. **A**—40-day-old plants grown in soil under control conditions (24 °C, 40 days, top); bottom: plants grown under control conditions (24 °C, 20 days) followed by moderate heat exposure (36 °C, 20 days). **B**—the relative length of plants grown under heat exposure (%). The control (WT) and transformed native (CPK1-OE), mutant inactive (KJM4-OE), and constitutively active (KJM23-OE) forms of the *AtCPK1* gene tobacco plants were grown in soil with regular watering. The data were obtained from 3 independent experiments with 10 replicates and are presented as the mean ± standard error of the mean. Asterisks above the error bars indicate statistically significant mean differences ($P < 0.05$, Fisher's LSD).

senescence. Similarly, heat stress affected the growth of KJM4-OE plants. Transformation with the native form of the *AtCPK1* gene did not increase resistance to heat stress (Figs. 6 and 7). The overexpression of the constitutively active form of the *AtCPK1* gene led to a significant increase in tolerance to heat stress in KJM23-OE plants. The growth of the KJM23-OE plants was unaffected by slight heat (Fig. 6A and B), whereas intense heat exposure at 42 °C inhibited KJM23-OE plant growth by 20% (Fig. 6A–C).

We also investigated the response of tobacco plants growing *in vitro* to heat shock. Interestingly, tobacco plants growing in soil were more tolerant to 42 °C than were plants growing *in vitro*. Thirty-four-day-old WT and transgenic tobacco plants grown *in vitro* were exposed to 42 °C as were the corresponding soil plants. However, after 5 days of heat treatment, the WT, KJM4-OE and CPK1-OE plants significantly senesced, whereas the KJM23-OE plants were green (Fig. 8, A). We analysed the relative NCC/DNCC content in the treated and untreated plants and revealed that after heat shock, the NCC/DNCC content in the WT, KJM4-OE and CPK1-OE plants increased more than 10-fold, whereas the NCC/DNCC content in KJM23-OE did not change (Fig. 8, B). These results indicate that overexpression of the calcium-independent form of the *AtCPK1* gene mitigated heat-induced senescence. Moreover, the tolerance of KJM23-OE to long-term heat stress may be related to the KJM23-mediated stabilization of heat-induced senescence. To clarify these aspects, we further investigated the biosynthesis of the main senescence-associated hormone ABA under thermal stress.

3.5. Baseline and thermoinduced ABA biosynthesis in AtCPK1-transformed N. tabacum

Next, we studied the expression of the genes encoding ABA biosynthesis enzymes in WT and transgenic *N. tabacum* plants. The main group of ABA biosynthesis enzymes is 9-cis-epoxycarotenoid dehydrogenases (NCEDs). In Arabidopsis plants, the AtNCED3 isoform was shown to promote stress-induced ABA biosynthesis (Iuchi et al., 2001). We selected two isoforms of the tobacco 9-cis-epoxycarotenoid dehydrogenase genes, *NtNCED1* and *NtNCED3*, which are most closely related to *AtNCED3*. Analysis of the expression of the *NtNCED1* and *NtNCED3* genes was carried out on 40-day-old micropropagated plants growing *in vitro*. In addition, the analysis was also carried out under intense short-term stresses: cold (4 °C) and heat (42 °C) for 1 h. We have shown that under control conditions, the expression of the *NtNCED3* gene is more than 6 times greater in KJM23-OE plants than in other plant variants. However, no difference in the expression of this isoform was found among the WT, KJM4-OE, and CPK1-OE plants. The expression of the *NtNCED1* gene was similar in all the tested plants under controlled conditions (Fig. 9). In the WT plants, cold and heat treatments had no effect on the expression of the *NtNCED1* gene. Cold stress led to an increase in *NtNCED3* expression of up to 5-fold. Exposure to intense heat stress for 1 h resulted in a significant (10–12-fold) increase in the expression of the *NtNCED3* gene in the WT, KJM4-OE, and CPK1-OE plants. In contrast, in the KJM23-OE plants, we observed a stable decrease in the expression of the *NtNCED3* isoform (Fig. 9).

Next, we confirmed the inhibitory effect of the constitutively active form of the *AtCPK1* gene (KJM23 form) on the biosynthesis of ABA in the early stage of heat stress. The heat-mediated modulation of ABA was measured using a highly sensitive and reproducible ELISA method with modified protocols for sample preparation. An HPLC−tandem mass spectrometry (HPLC−MS/MS) method was used to confirm successful ABA extraction. The ABA standard solution (10 ng/ml) and WT extract were analysed under the same conditions. The retention times and MS/MS fragmentation patterns of the target compounds from both samples were similar (Fig. 10, A) and consistent with previously published data (Veremeichik et al., 2022a). Using ELISA, we analysed concentrated extracts of 40-day-old WT and transgenic tobacco plants grown under control conditions and after heat shock treatment (42 °C for 1 h). The experiments were repeated four times with the same results. Therefore, the heat shock-induced differences in ABA levels match the differences observed in the expression of the *NCED3* gene (Figs. 9, 10, B).

3.6. Thermoinduced expression of senescence-associated ABA-dependent SAG12 and SA-dependent ACD6 genes in AtCPK1-expressing tobacco plants

Thus, we have shown the ability of the modified constitutively active calcium-independent form of AtCPK1 to activate the biosynthesis of baseline ABA and downregulate ABA biosynthesis under thermal stress. As a result, we observed the prevention of thermoinduced chlorophyll degradation in KJM23-OE plants. Next, we studied the possible mechanisms of the described processes. In general, stress-induced senescence accompanied by chlorophyll degradation is regulated through the ABA signalling pathway (Asad et al., 2019). Previously, CPK1 was shown to activate the expression of the senescence associated gene *SAG12* (Balazadeh et al., 2010) through phosphorylation of the senescence master regulator TF ORE1 (Durian et al., 2020a,bA). The ORE1-SAG12 system is strongly regulated by ABA (Matallana-Ramirez et al., 2013) and ROS (Garapati et al., 2015). In addition, SA-mediated ACD6 (ACCELERATED CELL DEATH 6) also regulates natural leaf senescence (Jasinski et al., 2021). To date, the role and function of this protein have remained unknown because its biochemical mechanism of action is

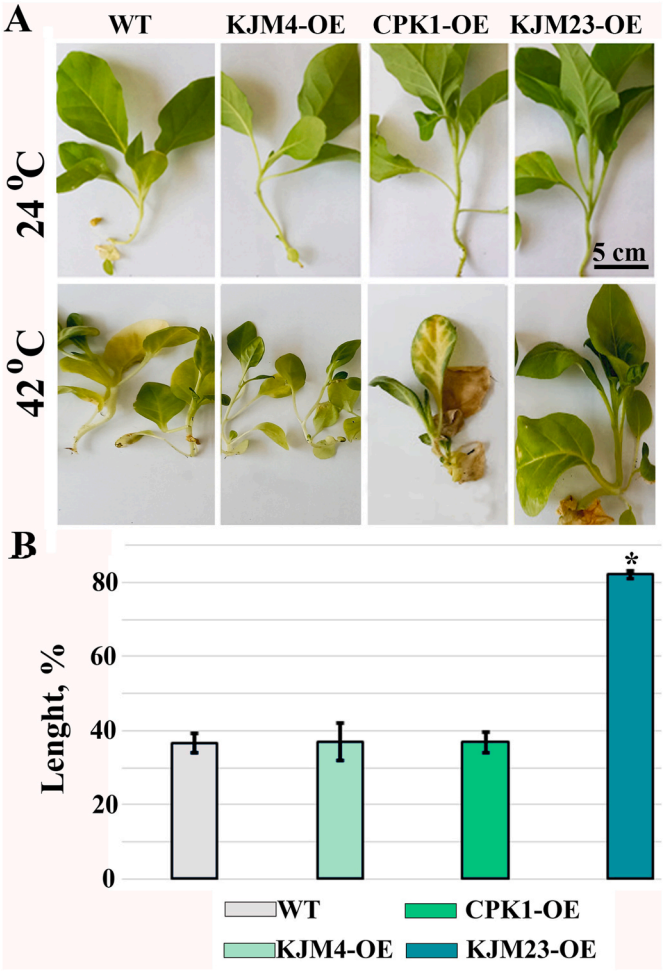

Fig. 7. Effects of intense heat stress on the growth of *N. tabacum* plants. **A**—50-day-old plants grown in soil under control conditions (24 °C, 50 days, top); bottom: plants grown under control conditions (24 °C, 30 days) followed by moderate heat exposure (42 °C, 20 days). **B**—the relative length of the plants under heat exposure (%). The control (WT) and transformed native (CPK1-OE), mutant inactive (KJM4-OE), and constitutively active (KJM23-OE) forms of the *AtCPK1* gene tobacco plants were grown in soil with regular watering. The data were obtained from 3 independent experiments with 10 replicates and are presented as the mean ± standard error of the mean. Asterisks above the error bars indicate statistically significant mean differences ($P < 0.05$, Fisher's LSD).

unclear. However, ACD6 is known to be part of the positive and negative regulatory loop of SA signalling and plays an important role in the regulation of calcium channels (Chen et al., 2023). Research in this area is also important because CPK1 has previously been shown to directly regulate SA signalling by activating SAR (Coca and San Segundo, 2010; Veremeichik et al., 2023a). Thus, to clarify the process of heat-induced senescence and the role of Ca^{2+} and CPK1 in this process, we examined the basal and thermoinduced expression levels of the *SAG12* and *ACD6* genes.

Under control conditions, the expression of the SA-dependent *ACD6* gene increased more than 5-fold in KJM23-OE plants compared with WT, KJM4-OE, and CPK1-OE plants (Fig. 8). Compared with that in the WT and KJM4-OE plants, the expression of the ABA-dependent *SAG12* gene was upregulated in both the CPK1-OE and KJM23-OE plants. However, in the CPK1-OE plants, the *SAG12* expression level did not increase by more than twofold, whereas in the KJM23-OE plants, it increased by more than fivefold compared with that in the WT plants. Short-term cold treatment led to an increase in *SAG12* and *ACD6* gene expression in the WT, KJM4-OE, and CPK1-OE plants and an almost fourfold decrease in the KJM23-OE plants. Heat treatment did not affect *SAG12* or *ACD6* gene expression more than twofold in the WT, KJM4-OE, or CPK1-OE plants. Moreover, the expression of the *SAG12* and *ACD6* genes was almost completely inhibited in the KJM23-OE plants under short-term heat treatment (Fig. 8).

3.7. Baseline and thermoinduced expression of HSF genes in AtCPK1-expressing tobacco plants

Previously, we reported differential regulation of heat shock factor (*HSF*) gene expression in WT and *AtCPK1*-transformed tobacco plants under salinity treatment (Veremeichik et al., 2021b). In the present work, we examined the expression of *HSF* genes under temperature stress to elucidate AtCPK1-mediated cold and heat tolerance. We analysed the expression of the master regulator *NtHSFA1* and the downstream isoforms *NtHSFA2* and *NtHSFA3* in WT plants and in plants expressing the native and modified forms of the *AtCPK1* gene after short-term intensive cold and heat treatments (Fig. 8). Real-time PCR analysis revealed that the expression of *NtHSFA2* was strongly upregulated at the early stage of intensive heat treatment. However, the expression of *NtHSFA1* did not significantly change in the WT, KJM4-OE, CPK1-OE, or KJM23-OE plants under heat stress conditions. Moreover, the expression of *NtHSFA3* decreased under heat stress in the WT, KJM4-OE, and CPK1-OE plants but not in the KJM23-OE plants compared to untreated WT plants. Cold stress led to a slight increase only in *NtHSFA1* gene expression.

Under control conditions, the expression of the *NtHSF1* gene was significantly greater in CPK1-OE plants than in WT plants. However, under cold and heat treatments, the expression of the *NtHSF1* gene was the same in the WT and CPK1-OE plants. However, neither cold nor heat stress significantly affected the expression of *NtHSF1* in the KJM23-OE plants. The overexpression of the native and constitutively active forms of the *AtCPK1* gene led to an increase in heat-induced *NtHSF2*

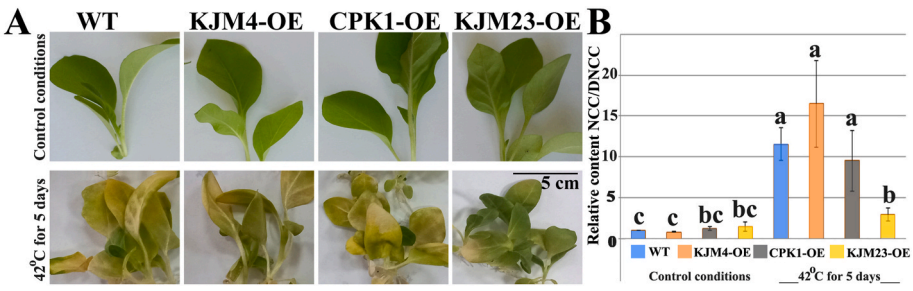

Fig. 8. Heat-induced accumulation of NCC/DNCC chlorophyll catabolites in *N. tabacum* plants. Morphology (**A**) and relative content of NCC/DNCC (**B**) in extracts of 40-day-old tobacco plants grown *in vitro* under unstressed conditions (24 °C, top) and after heat treatment at 42 °C for 5 days (bottom): the control (WT), transformed native (CPK1-OE), mutant inactive (KJM4-OE), and constitutively active (KJM23-OE) forms of the *AtCPK1* gene. The data were obtained from 3 independent experiments and are presented as the mean ± standard error of the mean. The different letters above the error bars indicate statistically significant differences ($P < 0.05$, Fisher's LSD).

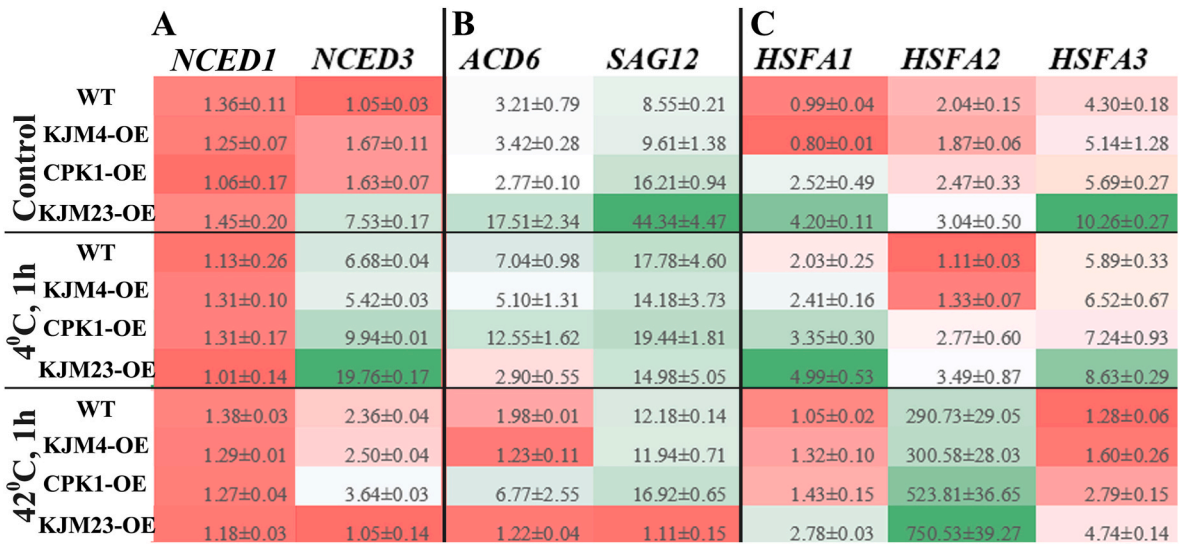

Fig. 9. Expression of the *NtNCEDs*, *NtHSFs*, and *NtSAG12* genes in *N. tabacum* plants under different temperature treatments. Forty-four-day-old, *in vitro*-grown the control (WT), transformed native (CPK1-OE), mutant inactive (KJM4-OE), and constitutively active (KJM23-OE) forms of the *AtCPK1* gene were subjected to temperature stress (4 °C and 42 °C) for 1 h. All stress treatments were repeated three times in three independent experiments (biological replicates), and qPCR measurements of each biological replicate were performed in three technical replicates. The data are presented as a heatmap calculated as $2^{-\Delta\Delta Ct}$ from the qPCR data. Different colours indicate significantly different means ($P < 0.05$), Fisher's LSD. (For interpretation of the references to colour in this figure legend, the reader is referred to the Web version of this article.)

gene expression of more than two and three times, respectively. In summary, overexpression of the constitutively active form of the *AtCPK1* gene (KJM23) led to an increase in baseline and heat- or cold-induced *NtHSF* gene expression, whereas the native form of the gene was not affected by heat stress. The expression of the modified, nonactive form of the *AtCPK1* gene did not differ from that of the WT.

4. Discussion

More than 30 years ago, Harper and Huang obtained mutant versions of the AtCPK1 gene *via* site-directed mutagenesis (Harper et al., 1994; Huang et al., 1996). These were biochemical investigations at the time of the autoinhibitory domain's subdomain structure and its ability to control CDPK activity. By altering the pseudosubstrate autoinhibition subdomain, constitutive activity is conferred upon the enzyme by preventing its reliance on calcium ion oscillations caused by stress. This imitation of stable stress leads to an increase in the threshold of sensitivity to adverse external influences. A modification in the calmodulin-like domain binding subdomain completely blocks enzyme activity. In the present work, the effects of the overexpression of two mutant forms of the *AtCPK1* gene on thermotolerance were analysed in comparison with those of native *AtCPK1*. We have previously shown that AtCPK1-KJM23 is more effective than the native form in stimulating the biosynthesis of phytoalexins in transformed cell cultures (Shkryl et al., 2011, 2016; Veremeichik et al., 2016).

Hormone profiling. First, we analysed the levels of endogenous SA, ABA, and IAA using a high-precision, high-resolution system. However, we were unable to detect an increase in SA, as expected, in either CPK1-OE or KJM23-OE plants. The obtained data contradict previous results (Coca and San Segundo, 2010; Veremeichik et al., 2023a). It can be assumed that a more detailed analysis of SA in terms of plant growth dynamics is needed. However, we detected a significant increase in ABA in KJM23-OE plants. This finding also indicates the need for a detailed analysis of hormonal status over time since ABA and SA are antagonistic agents (Cao et al., 2011; Nahar et al., 2012). The main external indicator of an increased level of endogenous ABA is the inhibition of seed germination (Ali et al., 2021; Schopfer et al., 1979). We investigated how the overexpression of native and modified forms of the *AtCPK1* gene affects seed germination. In *in vitro* experiments, we detected a significant delay in KJM23-OE germination until day 4. Subsequently, seed germination levelled off.

Another important manifestation of increased endogenous ABA is increased sensitivity to exogenous ABA. Both exogenous and endogenous ABA positively regulate natural aging processes and stress-induced senescence. This is expressed in the more intense senescence-associated degradation of chlorophyll (Ren et al., 2018). We analysed the content of chlorophyll catabolites in WT and transgenic plants under normal conditions and under exogenous ABA treatment. The analysis revealed that ABA-induced senescence is much more intense in plants transformed with the native and constitutively active forms of the *AtCPK1* gene. This finding indicates the involvement of Ca^{2+} in the process of ABA-induced senescence, which does not allow us to determine the difference between the native and constitutively active forms of the *AtCPK1* gene. These findings are consistent with the previously established CPK1-mediated activation of ORE1, one of the most important master regulators of ABA-dependent PCD and senescence (Durian et al., 2020a,b).

Cold stress. It is yet unclear how Ca^{2+} and calcium-dependent protein kinases contribute to thermotolerance. In brief, resistance to acute cold stress is increased by the overexpression of different CDPK gene isoforms (Almadanim et al., 2017; Liu et al., 2018; Lv et al., 2018). It is unknown how CDPK functions in low-temperature cultivation and long-term cold stress tolerance (Dekomah et al., 2022). Nonetheless, there has been enough research on the beneficial effect that intracellular Ca^{2+} has on controlling cold resistance. Both tobacco plants, which are susceptible to cold, and *Arabidopsis* plants, which can withstand cold, instantaneously increase the cytosolic Ca^{2+} concentration upon cold shock. Therefore, cold memory may be enhanced during acclimatization by altering calcium signalling (Knight et al., 1996; Song et al., 2008). Changes in intracellular Ca^{2+} are influenced by the frequency and duration of cold treatments. Furthermore, repeated cold treatments guarantee the development of "cold memory" by reducing the amount of intracellular Ca^{2+} influx caused by cold (Plieth et al., 2002). Genes involved in the Ca^{2+} signalling pathway and in plant reactions to cold stress are induced to be expressed when there is an external supply of Ca^{2+}. Stress tolerance is ultimately enhanced by increased expression of genes related to cold sensitivity and calcium signalling, which also preserve the cellular redox equilibrium and photosynthetic rates (Malko et al., 2023).

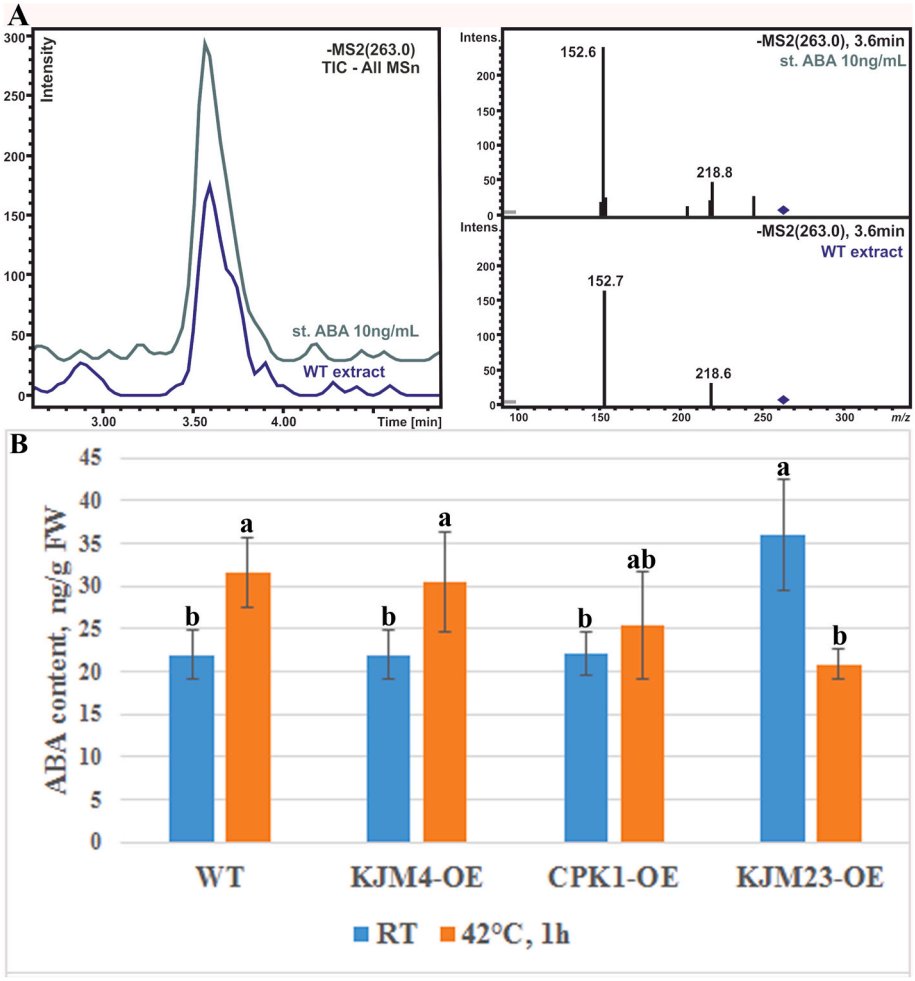

Fig. 10. Heat-induced accumulation of ABA in *N. tabacum* plants. Targeted HPLC–MS/MS determination of ABA in WT extracts (**A**), depicting the total ion current chromatograms of all product ions from precursors at *m/z* 263 (left) and fragment-ion MS/MS spectra obtained from the tops of the peaks (right). The ABA content (measured using ELISA, **B**) in untreated and heat-treated (42 °C for 1 h) forty-day-old, *in vitro*-grown control (WT), transformed native (CPK1-OE), mutant inactive (KJM4-OE), and constitutively active (KJM23-OE) forms of the *AtCPK1* gene in tobacco plants. The different letters above the error bars indicate statistically significant differences ($P < 0.05$, Fisher's LSD).

Therefore, it is anticipated that overexpressing CDPK will greatly increase tolerance to prolonged cold stress. However, we were unable to locate such data. It is likely that antagonistic interactions between Ca^{2+} and other signalling systems prevent Ca^{2+} from having beneficial effects during extended periods of cold stress, which decreases the effectiveness of transformation by calcium-dependent protein kinases.

However, in this study, we showed that plants transformed with a constitutively active form of the *AtCPK1* gene were significantly more resistant to long-term cold stress than plants transformed with the native form of the gene. Long-term (30-day) low-temperature treatment led to a 4-fold decrease in the growth of the control plants. The overexpression of the native form of the *AtCPK1* gene slightly but significantly increased resistance by no more than 20%. Moreover, the effect was shown both during seed germination and during the long-term cultivation of plants. Moreover, plants expressing the mutant constitutively active form of the *AtCPK1* gene were two times more resistant to cold than were the control plants. Overexpression of the native form of the *AtCPK1* gene led to weak but significant resistance to long-term cold (12 °C) during seed germination. Moreover, low temperature did not have an inhibitory effect on the germination of the KJM23-OE plants. Thus, we can conclude that the native form of *AtCPK1* confers cold tolerance and that inactivation of the autoinhibitory domain enhances this effect. However, notably, in this case, the effect of the expression of the native form of the gene on cold resistance is very weak. Thus, we have shown for the first time that direct inactivation of the autoinhibitory domain makes CDPK a powerful tool for producing cold-tolerant plants.

Heat stress. Crop production is facing more serious challenges due to global warming. The average world temperature is predicted to increase by approximately 1 °C by 2025, according to the Intergovernmental Panel on Climate Change (IPCC), which projected that it will increase at a rate of 0.3 °C over the course of a decade (Jones et al., 1999). Heat stress is a major danger to crop output worldwide because it disrupts cellular homeostasis, which ultimately results in stunted growth and even death (Hall, 2000). Studies (Ray et al., 2007; Romeis et al., 2001; Dubrovina et al., 2013; Dong et al., 2020; Veremeichik et al., 2022b) have demonstrated that some isoforms of the *CDPK* genes react to short, severe heat stress. Short-term (2–48 h) acute (42 °C) thermal stress increases the expression of 4 of the 19 isoforms of the *CDPK* genes of the wild Chinese grape *V. pseudoreticulata* (Zhang et al., 2015). Compared with cultivated soybeans, wild soy presented considerably greater increases in *GmCDPK5* and *GmCDPK10* expression under extreme short-term stress (Veremeichik et al., 2023a). The activation of protective mechanisms in *CDPK*-overexpressing plants in response to short-term heat treatment has also been shown (Tan et al., 2011; Wang and Song, 2014). Increased heat resistance should result from AtCPK28's direct phosphorylation of the stress marker enzyme APX2 under heat stress (Hu et al., 2021). Additionally, it has been demonstrated that the *cdpk* mutant has less heat tolerance (Wei et al., 2023).

Nevertheless, there is no evidence that plants that overexpress CDPK directly have greater heat tolerance (Dekomah et al., 2022). There are many contradictory findings regarding the function of Ca^{2+} in thermotolerance. The unclear role of Ca^{2+} in the response of cells to heat stress may explain why CDPKs are unable to develop tolerance to long-term heat stress in *CDPK*-overexpressing plants. Heat-induced Ca^{2+} influx was subsequently shown to have a cytotoxic effect (Wang et al., 2009). In addition, Ca^{2+} may regulate the development of programmed cell death (PCD). Thus, Ca^{2+} clearly plays a dual role in plant responses to elevated temperatures. On the one hand, it activates the expression of heat shock proteins (HSPs) and may protect the plant from death; on the other hand, it can stimulate plant death. It can be assumed that feedback loops block the possible positive effect of the CDPK. Phosphorylation-regulated Ca^{2+} channels or Ca^{2+}-induced phosphorylation-dependent pathways can be blocked through currents or the activation of phosphatases. This process may involve antagonism of the SAR and ABA signalling systems (Yasuda et al., 2008). We showed that *AtCPK1* overexpression in tobacco has no effect on resistance or sensitivity to heat stress. Moreover, the expression of the modified AtCPK1 form, which is independent of fluctuations in intracellular Ca^{2+} levels, significantly increases resistance to prolonged heat exposure. However, the role of intracellular Ca^{2+} in the regulation of heat tolerance is currently poorly understood. On the basis of the data obtained, inactivation of the CDPK autoinhibitory domain is a promising tool for making plants resistant to temperature stress.

4.1. Heat-induced senescence

On the basis of the obtained molecular and biochemical data, we propose the following model of the role of the CDPK under heat stress (Fig. 11). During the early stages of heat exposure, the intracellular Ca^{2+} concentration increases, which triggers cascades regulated by CDPK. However, later, Ca^{2+} levels decrease, which blocks CDPK from functioning. In turn, heat-induced excess ABA triggers chlorophyll catabolism (Kane and McAdam, 2023), which reduces the physiological load under short-term exposure but leads to plant death under long-term and intense heat stress (Song et al., 2016). We showed that the constitutively active form of AtCPK1 normally activates ABA biosynthesis, but a decrease in ABA content was detected upon heat exposure. As a consequence, a decrease in *SAG12* expression was observed. As a result, the leaves of KJM23-OE plants were much less yellow than those of WT plants under heat stress. We can assume that this effect is achieved through the CPK-dependent activation of SA signalling. SA and ABA are known to be antagonistic, and the activation of SAR inhibits ABA signalling (Cao et al., 2011; Nahar et al., 2012). On the one hand, this hypothesis is supported by previously obtained data on CPK-dependent activation of SA signalling, both SA biosynthesis (Coca and San Segundo, 2010) and activation of the expression of proteins associated with SAR (Veremeichik et al., 2023a). On the other hand, this hypothesis is confirmed by the data obtained in this work. We observed a decrease in the expression of the SA-dependent protease ACD6. ACD6 is involved in the feedback regulation of SA signalling and mediates the hypersensitivity response and PCD (Rate et al., 1999). Thus, further research in this area involves a detailed study of the biosynthesis and signalling of ABA and SA during long-term heat stress and the role of the native and constitutively active forms of AtCPK1 in these processes.

5. Conclusion

By altering the pseudosubstrate autoinhibition subdomain, constitutive activity is conferred upon the enzyme by preventing its reliance on calcium ion oscillations caused by stress. We have shown for the first time that direct inactivation of the autoinhibitory domain makes CDPK a powerful tool for producing cold- and heat-tolerant plants. We showed that the constitutively active form of AtCPK1 normally activates ABA biosynthesis, but a decrease in ABA content was detected upon heat exposure. As a consequence, a decrease in SAG12 expression was shown. As a result, the leaves of KJM23-OE plants were much less yellow than those of WT plants under heat stress. We can assume that this effect is achieved through the CPK-dependent activation of SA signalling. SA and ABA are known to be antagonistic, and the activation of SAR inhibits ABA signalling.

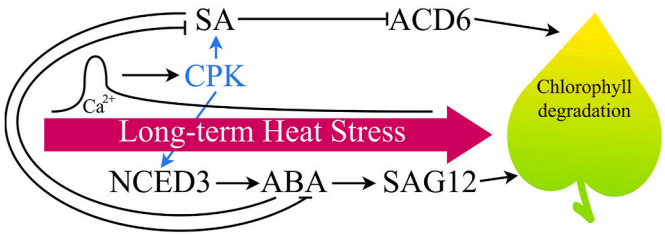

Fig. 11. Proposed model of the role of the CDPK under heat stress. During the early stages of heat exposure, the intracellular calcium concentration increases, which triggers cascades regulated by CDPK. Later, calcium levels decrease, which blocks CDPK; heat-induced excess ABA triggers chlorophyll catabolism (Kane and McAdam, 2023). SA and ABA are known to be antagonistic (Cao et al., 2011; Nahar et al., 2012). ACD6 is involved in the feedback regulation of SA signalling and mediates the hypersensitivity response and PCD (Rate et al., 1999).

CRediT authorship contribution statement

G.N. Veremeichik: Writing – review & editing, Writing – original draft, Visualization, Validation, Supervision, Project administration, Methodology, Investigation, Funding acquisition, Formal analysis, Data curation, Conceptualization. **O.A. Tikhonova:** Methodology, Investigation, Formal analysis. **V.P. Grigorchuk:** Methodology, Investigation, Formal analysis. **S.A. Silantieva:** Investigation, Methodology, Formal Analysis. **E.V. Brodovskaya:** Methodology, Investigation, Formal analysis. **D.V. Bulgakov:** Methodology, Investigation, Formal analysis. **V.P. Bulgakov:** Resources.

Funding

Financial support was provided by the Russian Science Foundation, Grant no. 24-24-00005 (G.N. Veremeichik).

Declaration of competing interest

The authors declare that they have no known competing financial interests or personal relationships that could have appeared to influence the work reported in this paper.

Acknowledgements

The analyses described in this work were performed *via* equipment from the Instrumental Centre for Biotechnology and Gene Engineering at the Federal Scientific Centre of East Asia Terrestrial Biodiversity of the Far East Branch of the Russian Academy of Sciences.

Appendix A. Supplementary data

Supplementary data to this article can be found online at https://doi.org/10.1016/j.jplph.2024.154413.

Data availability

Data will be made available on request.

References

Ali, F., Qanmber, G., Li, F., Wang, Z., 2021. Updated role of ABA in seed maturation, dormancy, and germination. J. Adv. Res. 35, 199–214. https://doi.org/10.1016/j.jare.2021.03.011.

Almadanim, M.C., Goncalves, N.M., Rosa, M.T.G., Alexandre, B.M., Cordeiro, A.M., Rodrigues, M., Saibo, N.J.M., Soares, C.M., Romao, C.V., Oliveira, M.M., Abreu, I.A., 2017. The rice cold-responsive calcium-dependent protein kinase *OsCPK17* is regulated by alternative splicing and posttranslational modifications. Biochim. Biophys. Acta Mol. Cell Res. 1865 (2), 231–246. https://doi.org/10.1016/j.bbamcr.2017.10.010.

Asad, M.A.U., Zakari, S.A., Zhao, Q., Zhou, L., Ye, Y., Cheng, F., 2019. Abiotic stresses intervene with ABA signaling to induce destructive metabolic pathways leading to death: premature leaf senescence in plants. IJMS 20 (2), 256. https://doi.org/10.3390/ijms20020256.

Baek, E., Yoon, J.Y., Palukaitis, P., 2017. Validation of reference genes for quantifying changes in gene expression in virus-infected tobacco. Virology 510, 29–39. https://doi.org/10.1016/j.virol.2017.06.029.

Balazadeh, S., Siddiqui, H., Allu, A.D., Matallana-Ramirez, L.P., Caldana, C., Mehrnia, M., Zanor, M.I., Köhler, B., Mueller-Roeber, B., 2010. A gene regulatory network controlled by the NAC transcription factor ANAC092/AtNAC2/ORE1 during salt-promoted senescence. Plant J. 62 (2), 250–264. https://doi.org/10.1111/j.1365-313X.2010.04151.x.

Berghold, J., Eichmüller, C., Hörtensteiner, S., Kräutler, B., 2004. Chlorophyll breakdown in tobacco: on the structure of two nonfluorescent chlorophyll catabolites. Chem Biodiv 1 (4), 657–668. https://doi.org/10.1002/cbdv.200490057.

Bredow, M., Monaghan, J., 2019. Regulation of plant immune signaling by calcium-dependent protein kinases. MPMI (Mol. Plant-Microbe Interact.) 32 (1), 6–19. https://doi.org/10.1094/MPMI-09-18-0267-FI.

Breeze, E., Harrison, E., McHattie, S., Hughes, L., Hickman, R., Hill, C., Kiddle, S., Kim, Y. S., Penfold, C.A., Jenkins, D., Zhang, C., Morris, K., Jenner, C., Jackson, S., Thomas, B., Tabrett, A., Legaie, R., Moore, J.D., Wild, D.L., Ott, S., Rand, D., Beynon, J., Denby, K., Mead, A., Buchanan-Wollaston, V., 2011. High-resolution temporal profiling of transcripts during *Arabidopsis* leaf senescence reveals a distinct chronology of processes and regulation. Plant Cell 23 (3), 873–894. https://doi.org/10.1105/tpc.111.083345.

Cao, F.Y., Yoshioka, K., Desveaux, D., 2011. The roles of ABA in plant–pathogen interactions. J. Plant Res. 124 (4), 489–499. https://doi.org/10.1007/s10265-011-0409-y.

Chen, J., Li, L., Kim, J.H., Neuhäuser, B., Wang, M., Thelen, M., Hilleary, R., Chi, Y., Wei, L., Venkataramani, K., Exposito-Alonso, M., Liu, C., Keck, J., Barragan, A.C., Schwab, R., Lutz, U., Pei, Z.M., He, S.Y., Ludewig, U., Weigel, D., Zhu, W., 2023. Small proteins modulate ion-channel-like ACD6 to regulate immunity in *Arabidopsis thaliana*. Mol cell 83 (23), 4386–4397.e9. https://doi.org/10.1016/j.molcel.2023.10.030.

Chinnusamy, V., Zhu, J.K., Sunkar, R., 2010. Gene regulation during cold stress acclimation in plants. Meth Mol Biol 639, 39–55. https://doi.org/10.1007/978-1-60761-702-0_3.

Christ, B., Süssenbacher, I., Moser, S., Bichsel, N., Egert, A., Müller, T., Kräutler, B., Hörtensteiner, S., 2013. Cytochrome P450 CYP89A9 is involved in the formation of major chlorophyll catabolites during leaf senescence in *Arabidopsis*. Plant Cell 25 (5), 1868–1880. https://doi.org/10.1105/tpc.113.112151.

Christ, B., Hauenstein, M., Hörtensteiner, S., 2016. A liquid chromatography–mass spectrometry platform for the analysis of phyllobilins, the major degradation products of chlorophyll in *Arabidopsis thaliana*. Plant J. 88 (3), 505–518. https://doi.org/10.1111/tpj.13253.

Coca, M., San Segundo, B., 2010. *AtCPK1* calcium-dependent protein kinase mediates pathogen resistance in *Arabidopsis*. Plant J. 63, 526–540. https://doi.org/10.1111/j.1365-313X.2010.04255.

Costa, A., Navazio, L., Szabo, I., 2018. The contribution of organelles to plant intracellular Calcium signalling. JEXB 69 (17), 4175–4193. https://doi.org/10.1093/jxb/ery185.

Dekomah, S.D., Bi, Z., Dormatey, R., Wang, Y., Haider, F.U., Sun, C., Yao, P., Bai, J., 2022. The role of CDPKs in plant development, nutrient and stress signaling. Front. Genet. 13, 996203. https://doi.org/10.3389/fgene.2022.996203.

Dong, H., Wu, C., Luo, C., Wei, M., Qu, S., Wang, S., 2020. Overexpression of *MdCPK1a* gene, a calcium dependent protein kinase in apple, increase tobacco cold tolerance *via* scavenging ROS accumulation. PLoS One 15 (11), e0242139. https://doi.org/10.1371/journal.pone.0242139.

Dubrovina, A.S., Kiselev, K.V., Khristenko, V.S., 2013. Expression of calcium-dependent protein kinase (*CDPK*) genes under abiotic stress conditions in wild-growing grapevine *Vitis amurensis*. J. Plant Physiol. 170 (17), 1491–1500. https://doi.org/10.1016/j.jplph.2013.06.014.

Durian, G., Jeschke, V., Rahikainen, M., Vuorinen, K., Gollan, P.J., Brosché, M., Salojärvi, J., Glawischnig, E., Winter, Z., Li, S., Noctor, G., Aro, E.M., Kangasjärvi, J., Overmyer, K., Burow, M., Kangasjärvi, S., 2020a. Protein phosphatase 2A-B'γ controls *Botrytis cinerea* resistance and developmental leaf senescence. Plant Physiol 182 (2), 1161–1181. https://doi.org/10.1104/pp.19.00893.

Durian, G., Sedaghatmehr, M., Matallana-Ramirez, L., Schilling, S.M., Schaepe, S., Guerra, T., Herde, M., Witte, C., Mueller-Roeber, B., Schulze, W.X., Balazadeh, S., Romeis, T., 2020b. Calcium-dependent protein Kinase CPK1 controls cell death by *in vivo* phosphorylation of senescence master regulator ORE1. Plant Cell 32 (5), 1610–1625. https://doi.org/10.1105/tpc.19.00810.

Garapati, P., Xue, G.P., Munné-Bosch, S., Balazadeh, S., 2015. Transcription factor ATAF1 in arabidopsis promotes senescence by direct regulation of key chloroplast maintenance and senescence transcriptional cascades. Plant Physiol 3, 1122–1139. https://doi.org/10.1104/pp.15.00567.

Hall, A.E., 2000. Crop Responses to Environment. CRC press, Boca Raton, FL, USA. https://doi.org/10.1201/9781420041088.

Harper, J.F., Huang, J.F., Lloyd, S.J., 1994. Genetic identification of an autoinhibitor in CDPK, a protein kinase with a calmodulin-like domain. Biochem 33, 7267–7277. https://doi.org/10.1021/bi00189a031.

Horsch, R.B., Fry, J.E., Hoffmann, N.L., Eichholtz, D., Rogers, S.G., Fraley, R.T., 1985. A simple and general method for transferring genes into plants. Science 227, 1229–1231. https://doi.org/10.1126/science.227.4691.1229.

Hu, Z., Li, J., Ding, S., Cheng, F., Li, X., Jiang, Y., Yu, J., Foyer, C.H., Shi, K., 2021. The protein kinase CPK28 phosphorylates ascorbate peroxidase and enhances thermotolerance in tomato. Plant Physiol 186 (2), 1302–1317. https://doi.org/10.1093/plphys/kiab120.

Huang, J., Teyton, L., Harper, J.F., 1996. Activation of a Ca^{2+}-dependent protein kinase involves intramolecular binding of a calmodulin-like regulatory domain. Biochem 35 (40), 13222–13230. https://doi.org/10.1021/bi960498a.

Huang, K., Peng, L., Liu, Y., Yao, R., Liu, Z., Li, X., Yang, Y., Wang, J., 2017. Calcium-dependent protein kinase *AtCPK1* plays a positive role in salt/drought-stress response. Biochem. Biophys. Res. Commun. 498 (1), 92–98. https://doi.org/10.1016/j.bbrc.2017.11.175.

Iuchi, S., Kobayashi, M., Taji, T., Naramoto, M., Seki, M., Kato, T., Tabata, S., Kakubari, Y., Yamaguchi-Shinozaki, K., Shinozaki, K., 2001. Regulation of drought tolerance by gene manipulation of 9-cis-epoxycarotenoid dioxygenase, a key enzyme in abscisic acid biosynthesis in *Arabidopsis*. Plant J. 27 (4), 325–333. https://doi.org/10.1046/j.1365-313x.2001.01096.x.

Jasinski, S., Fabrissin, I., Masson, A., Marmagne, A., Lécureuil, A., Bill, L., Chardon, F., 2021. Accelerated cell death 6 acts on natural leaf senescence and nitrogen fluxes in *Arabidopsis*. Front plant sci 11, 611170. https://doi.org/10.3389/fpls.2020.611170.

Jones, P.D., New, M., Parker, D.E., Martin, S., Rigor, I.G., 1999. Surface air temperature and its changes over the past 150 years. Rev. Geophys. 37, 173–199. https://doi.org/10.1029/1999RG900002.

Kane, C.N., McAdam, S.A.M., 2023. Abscisic acid can augment, but is not essential for, autumnal leaf senescence. JEXB 74 (10), 3255–3266. https://doi.org/10.1093/jxb/erad089.

Kang, J., Yim, S., Choi, H., Kim, A., Lee, K.P., Lopez-Molina, L., Martinoia, E., Lee, Y., 2015. Abscisic acid transporters cooperate to control seed germination. Nature commun 6, 8113. https://doi.org/10.1038/ncomms9113.

Knight, H., Trewavas, A.J., Knight, M.R., 1996. Cold calcium signaling in *Arabidopsis* involves two cellular pools and a change in calcium signature after acclimation. Plant Cell 8 (3), 489–503. https://doi.org/10.1105/tpc.8.3.489.

Kudla, J., Batistic, O., Hashimoto, K., 2010. Calcium signals: the lead currency of plant information processing. Plant Cell 22 (3), 541–563. https://doi.org/10.1105/tpc.109.072686.

Lee, I.C., Hong, S.W., Whang, S.S., Lim, P.O., Nam, H.G., Koo, J.C., 2011. Age-dependent action of an ABA-inducible receptor kinase, RPK1, as a positive regulator of senescence in Arabidopsis leaves. Plant Cell Physiol. 52, 651–662. https://doi.org/10.1093/pcp/pcr026.

Li, G., Zhang, C., Zhang, G., Fu, W., Feng, B., Chen, T., Peng, S., Tao, L., Fu, G., 2020. Abscisic acid negatively modulates heat tolerance in rolled leaf rice by increasing leaf temperature and regulating energy homeostasis. Rice 13 (1), 18. https://doi.org/10.1186/s12284-020-00379-3.

Lim, P.O., Kim, H.J., Nam, H.G., 2007. Leaf senescence. Ann Rev Plant Biol 58, 115–136. https://doi.org/10.1146/annurev.arplant.57.032905.105316.

Liu, Y., Xu, C., Zhu, Y., Zhang, L., Chen, T., Zhou, F., Chen, H., Lin, Y., 2018. The calcium-dependent kinase *OsCPK24* functions in cold stress responses in rice. J Int Plant Biol 60, 173–188. https://doi.org/10.1111/jipb.12614.

Lv, X., Li, H., Chen, X., Xiang, X., Guo, Z., Yu, J., Zhou, Y., 2018. The role of calcium-dependent protein kinase in hydrogen peroxide, nitric oxide and ABA-dependent cold acclimation. JEXB 69 (16), 4127–4139. https://doi.org/10.1093/jxb/ery212.

Malko, M.M., Peng, X., Gao, X., Cai, J., Zhou, Q., Wang, X., Jiang, D., 2023. Effect of exogenous calcium on tolerance of winter wheat to cold stress during stem elongation stage. Plants 12 (21), 3784. https://doi.org/10.3390/plants12213784.

Matallana-Ramirez, L.P., Rauf, M., Farage-Barhom, S., Dortay, H., Xue, G.P., Dröge-Laser, W., Lers, A., Balazadeh, S., Mueller-Roeber, B., 2013. NAC transcription factor ORE1 and senescence-induced BIFUNCTIONAL NUCLEASE1 (BFN1) constitute a regulatory cascade in *Arabidopsis*. Mol. Plant 6 (5), 1438–1452. https://doi.org/10.1093/mp/sst012.

Mittler, R., Zandalinas, S.I., Fichman, Y., Van Breusegem, F., 2022. Reactive oxygen species signalling in plant stress responses. Nature reviews. Mol Cell Biol 23 (10), 663–679. https://doi.org/10.1038/s41580-022-00499-2.

Moser, S., Erhart, T., Neuhauser, S., Kräutler, B., 2020. Phyllobilins from senescence-associated chlorophyll breakdown in the leaves of basil (*Ocimum basilicum*) show increased abundance upon herbivore attack. J Agricul food chem 68 (27), 7132–7142. https://doi.org/10.1021/acs.jafc.0c02238.

Murashige, T., Skoog, F., 1962. A revised medium for rapid growth and bioassays with tobacco tissue culture. Plant Physiol 15, 473–497. https://doi.org/10.1111/j.1399-3054.1962.tb08052.x.

Nahar, K., Kyndt, T., Nzogela, Y.B., Gheysen, G., 2012. Abscisic acid interacts antagonistically with classical defense pathways in rice-migratory nematode interaction. New Phytol. 196 (3), 901–913. https://doi.org/10.1111/j.1469-8137.2012.04310.x.

Ng, L.M., Melcher, K., Teh, B.T., Xu, H.E., 2014. Abscisic acid perception and signaling: structural mechanisms and applications. Acta Pharmacol. Sin. 35 (5), 567–584. https://doi.org/10.1038/aps.2014.5.

Pérez-Gálvez, A., Roca, M., 2017. Phyllobilins. Stud. Nat. Prod. Chem. 52, 159–191. https://doi.org/10.1016/B978-0-444-63931-8.00004-7. Elsevier.

Plieth, C., Hansen, U.P., Knight, H., Knight, M.R., 2002. Temperature sensing by plants: the primary characteristics of signal perception and calcium response. Plant J. 18 (5), 491–497. https://doi.org/10.1046/j.1365-313x.1999.00471.x.

Rate, D.N., Cuenca, J.V., Bowman, G.R., Guttman, D.S., Greenberg, J.T., 1999. The gain-of-function Arabidopsis acd6 mutant reveals novel regulation and function of the salicylic acid signaling pathway in controlling cell death, defenses, and cell growth. Plant Cell 11 (9), 1695–1708. https://doi.org/10.1105/tpc.11.9.1695.

Ray, S., Agarwal, P., Arora, R., Kapoor, S., Tyagi, A.K., 2007. Expression analysis of calcium-dependent protein kinase gene family during reproductive development and abiotic stress conditions in rice (*Oryza sativa* L. ssp. indica). Mol. Genet. Genom. 278, 493–505. https://doi.org/10.1007/s00438-007-0267-4.

Ren, T., Wang, J., Zhao, M., Gong, X., Wang, S., Wang, G., Zhou, C., 2018. Involvement of NAC transcription factor SiNAC1 in a positive feedback loop via ABA biosynthesis and leaf senescence in foxtail millet. Planta 247 (1), 53–68. https://doi.org/10.1007/s00425-017-2770-0.

Resentini, F., Ruberti, C., Grenzi, M., Bonza, M.C., Costa, A., 2021. The signatures of organellar calcium. Plant Physiol 187 (4), 1985–2004. https://doi.org/10.1093/plphys/kiab189.

Romeis, T., Ludwig, A.A., Martin, R., Jones, J.D., 2001. Calcium-dependent protein kinases play an essential role in a plant defence response. EMBO J. 20, 5556–5567. https://doi.org/10.1093/emboj/20.20.5556.

Roychoudhury, A., Paul, S., Basu, S., 2013. Cross-talk between abscisic acid-dependent and abscisic acid-independent pathways during abiotic stress. Plant Cell Rep. 32 (7), 985–1006. https://doi.org/10.1007/s00299-013-1414-5.

Schopfer, P., Bajracharya, D., Plachy, C., 1979. Control of seed germination by abscisic acid: i. time course of action in *Sinapis alba L.* Plant Physiol 64 (5), 822–827. https://doi.org/10.1104/pp.64.5.822.

Shkryl, Y.N., Veremeichik, G.N., Bulgakov, V.P., Zhuravlev, Y.N., 2011. Induction of anthraquinone biosynthesis in *Rubia cordifolia* cells by heterologous expression of a calcium-dependent protein kinase gene. Biotechnol. Bioeng. 108 (7), 1734–1738. https://doi.org/10.1002/bit.23077.

Shkryl, Y.N., Veremeichik, G.N., Makhazen, D.S., Silantieva, S.A., Mishchenko, N.P., Vasileva, E.S., Fedoreyev, S.A., Bulgakov, V.P., 2016. Increase of anthraquinone content in *Rubia cordifolia* cells transformed by native and constitutively active forms of the *AtCPK1* gene. Plant Cell Rep. 9 (35), 19017. https://doi.org/10.1007/s00299-016-2005-z, 1916.

Song, W.Y., Zhang, Z.B., Shao, H.B., Guo, X.L., Cao, H.X., Zhao, H.B., Fu, Z.Y., Hu, X.J., 2008. Relationship between calcium decoding elements and plant abiotic-stress resistance. Int. J. Biol. Sci. 4 (2), 116–125. https://doi.org/10.7150/ijbs.4.116.

Song, Y., Xiang, F., Zhang, G., Miao, Y., Miao, C., Song, C.P., 2016. Abscisic acid as an internal integrator of multiple physiological processes modulates leaf senescence onset in *arabidopsis thaliana*. Front. Plant Sci. 7, 181. https://doi.org/10.3389/fpls.2016.00181.

Tan, W., Meng, Qw, Brestic, M., Olsovska, K., Yang, X., 2011. Photosynthesis is improved by exogenous calcium in heat-stressed tobacco plants. J. Plant Physiol. 168 (17), 2063–2071. https://doi.org/10.1016/j.jplph.2011.06.009.

Veremeichik, G.N., Shkryl, Y.N., Pinkus, S.A., Bulgakov, V.P., 2014. Expression profiles of calcium-dependent protein kinase genes (CDPK1-14) in Agrobacterium rhizogenes pRiA4-transformed calli of *Rubia cordifolia* under temperature- and salt-induced stresses. J. Plant Physiol. 171 (7), 467–474. https://doi.org/10.1016/j.jplph.2013.12.010.

Veremeichik, G.N., Grigorchuk, V.P., Shkryl, Y.N., Bulgakov, D.V., Silantieva, S.A., Bulgakov, V.P., 2016. Induction of resveratrol biosynthesis in *Vitis amurensis* cells by heterologous expression of the *Arabidopsis* constitutively active, Ca^{2+}-independent form of the *AtCPK1* gene. Process Biochem 54, 144–155. https://doi.org/10.1016/j.procbio.2016.12.026.

Veremeichik, G.N., Bulgakov, V.P., Shkryl, Y.N., Silantieva, S.A., Makhazen, D.S., Tchernoded, G.K., Mischenko, N.P., Fedoreyev, S.A., Vasileva, E.A., 2019. Activation of anthraquinone biosynthesis in long-cultured callus culture of *Rubia cordifolia* transformed with the *rolA* plant oncogene. J. Biotechnol. 306, 38–46. https://doi.org/10.1016/j.jbiotec.2019.09.007.

Veremeichik, G.N., Shkryl, Y.N., Gorpenchenko, T.Y., Silantieva, S.A., Avramenko, T.V., Brodovskaya, E.V., Bulgakov, V.P., 2021a. Inactivation of the auto-inhibitory domain in *Arabidopsis AtCPK1* leads to increased salt, cold and heat tolerance in the *AtCPK1*-transformed *Rubia cordifolia L* cell cultures. Plant Physiol Biochem 159, 372–382. https://doi.org/10.1016/j.plaphy.2020.12.031.

Veremeichik, G.N., Shkryl, Y.N., Silantieva, S.A., Gorpenchenko, T.Y., Brodovskaya, E.V., Yatsunskaya, M.S., Bulgakov, V.P., 2021b. Managing activity and Ca2+ dependence through mutation in the Junction of the *AtCPK1* coordinates the salt tolerance in transgenic tobacco plants. Plant Physiol Biochem 165, 104–113. https://doi.org/10.1016/j.plaphy.2021.05.026.

Veremeichik, G.N., Shkryl, Y.N., Rusapetova, T.V., Silantieva, S.A., Grigorchuk, V.P., Velansky, P.V., Brodovskaya, E.V., Konnova, Y.A., Khopta, A.A., Bulgakov, D.V., Bulgakov, V.P., 2022a. Overexpression of the A4-*rolB* gene from the pRiA4 of Rhizobium rhizogenes modulates hormones homeostasis and leads to an increase of flavonoid accumulation and drought tolerance in *Arabidopsis thaliana* transgenic plants. Planta 256 (1), 8. https://doi.org/10.1007/s00425-022-03927-x.

Veremeichik, G.N., Brodovskaya, E.V., Grigorchuk, V.P., Butovets, E.S., Lukyanchuk, L. M., Bulgakov, V.P., 2022b. ABA-dependent regulation of calcium-dependent protein kinase gene *GmCDPK5* in cultivated and wild soybeans. Life 12 (10), 1576. https://doi.org/10.3390/life12101576.

Veremeichik, G.N., Bulgakov, D.V., Konnova, Y.A., Brodovskaya, E.V., Grigorchuk, V.P., Bulgakov, V.P., 2023a. Proteome-level investigation of *Vitis amurensis* calli transformed with a constitutively active. Ca^{2+}-independent form of the Arabidopsis AtCPK1 gene Int J Mol Sci 24 (17), 13184. https://doi.org/10.3390/ijms241713184.

Veremeichik, G.N., Grigorchuk, V.P., Makhazen, D.S., Subbotin, E.P., Kholin, A.S., Subbotina, N.I., Bulgakov, D.V., Kulchin, Y.N., Bulgakov, V.P., 2023b. High production of flavonols and anthocyanins in *Eruca sativa (Mill) Thell* plants at high artificial LED light intensities. Food Chem. 408, 135216. https://doi.org/10.1016/j.foodchem.2022.135216.

Veselov, S.Y., Kudoyarova, G.R., Egutkin, N.L., Gyuli-Zade, V.Z., Mustafina, A.R., Kof, E. M., 1992. Modified solvent partitioning scheme providing increased specificity and rapidity of immunoassay for indole-3-acetic acid. Physiol Plant 86, 93–96. https://doi.org/10.1111/j.1399-3054.1992.tb01316.x.

Wang, C.T., Song, W., 2014. *ZmCK3*, a maize calcium-dependent protein kinase gene, endows tolerance to drought and heat stresses in transgenic *Arabidopsis*. J. Plant Biochem. Biotechnol. 23, 249–256. https://doi.org/10.1007/s13562-013-0208-8.

Wang, Y., Yu, Q., Tang, X., Wang, L., 2009. Calcium pretreatment increases thermotolerance of *Laminaria japonica* sporophytes. Prog. Nat. Sci. 19 (4), 435–442. https://doi.org/10.1016/J.PNSC.2008.07.016.

Watillon, B., Kettmann, R., Boxus, P., Burny, A.R., 1993. Communication a calcium/calmodulin-binding serine/threonine protein kinase homologous to the mammalian type calcium/calmodulin-dependent protein kinase 1s expressed in plant cells. Plant Physiol 101 (4), 1381–1384. https://doi.org/10.1104/pp.101.4.1381.

Wei, J.-T., Hou, Z.-H., Wang, Y., Hao, J.-M., Wang, J., Wang, W., Wang, W., Wang, D.-M., Xu, Z.-S., Song, X., Wang, F., Li, R., 2023. Foxtail millet *SiCDPK7* gene enhances tolerance to extreme temperature stress in transgenic plants. Env Exp Bot 207, 105197. https://doi.org/10.1016/j.envexpbot.2022.105197.

White, P.J., Broadley, M.R., 2003. Calcium in plants. Ann. Bot. 92 (4), 487–511. https://doi.org/10.1093/aob/mcg164.

Xing, T., Wang, X.-J., Malk, K., Mikl, B., 2001. Ectopic expression of an *Arabidopsis* calmodulin-like domain protein kinase-enhanced NADPH oxidase activity and oxidative burst in tomato protoplasts. MPMI (Mol. Plant-Microbe Interact.) 14 (10), 1261–1264. https://doi.org/10.1094/MPMI.2001.14.10.1261.

Yasuda, M., Ishikawa, A., Jikumaru, Y., Seki, M., Umezawa, T., Asami, T., Maruyama-Nakashita, A., Kudo, T., Shinozaki, K., Yoshida, S., Nakashita, H., 2008. Antagonistic interaction between systemic acquired resistance and the abscisic acid-mediated abiotic stress response in *Arabidopsis*. Plant Cell 20 (6), 1678–1692. https://doi.org/10.1105/tpc.107.054296.

Yip Delormel, T., Boudsocq, M., 2019. Properties and functions of calcium-dependent protein kinases and their relatives in *Arabidopsis thaliana*. New Phytol. 224, 585–604. https://doi.org/10.1111/nph.16088.

Zacarias, L., Reid, M.S., 1990. Role of growth regulators in the senescence of *Arabidopsis thaliana* leaves. Physiol Plant 80, 549–554. https://doi.org/10.1111/j.1399-3054.1990.tb05677.x.

Zhang, K., Han, Y.T., Zhao, F.L., Hu, Y., Gao, Y.R., Ma, Y.F., Zheng, Y., Wang, Y.J., Wen, Y.Q., 2015. Genome-wide identification and expression analysis of the *CDPK* gene family in grape, *Vitis* spp. BMC Plant Biol. 15, 164. https://doi.org/10.1186/s12870-015-0552-z.